

PROJECT ADMINISTRATION DATA SHEET



ORIGINAL



REVISION NO.

Subject No.

~~E-26-675~~

E-25-678 - Rev#7

DATE: 5/25/81

Subject Director:

Dr. Glenn Bateman

/ Dr. W. M. Stacey

School, EES,

Nuclear Engineering

Sponsor:

Department of Energy; Oak Ridge Operations; Oak Ridge, TN 37830

e Agreement:

Contract DE-AS05-81ER53117

rd Period: From

4/1/81

To

11/30/81

(Performance)

(Reports)

nsor Amount:

\$12,000

t Sharing:

None

le:

Saturated Tearing Modes in Tokamaks with Divertors

ADMINISTRATIVE DATA

OCA CONTACT

William F. Brown

x 4820

Sponsor Technical Contact:

Sponsor Admin./Contractual Contact:

W. A. Mynatt, Chief, Contract Management Branch,

Procurement & Contracts Division; Department of Energy; Oak Ridge Operations; P. O.

Box E; Oak Ridge, TN 37830

orts: See Deliverable Schedule

Security Classification:

ense Priority Rating:

RESTRICTIONS

Attached Government

Supplemental Information Sheet for Additional Requirements.

vel: Foreign travel must have prior approval - Contact OCA in each case. Domestic travel requires sponsor approval where total will exceed greater of \$500 or 125% of approved proposal budget category.

ipment: Title vests with GIT; however, none authorized/proposed.

REMARKS:

DISTRIBUTION TO:

Administrative Coordinator

Research Property Management

Accounting Office

Procurement/EES Supply Services

Research Security Services

Reports Coordinator (OCA)

Legal Services (OCA)

Library, Technical Reports

EES Research Public Relations (2

Project File (OCA)

Other:

SPONSORED PROJECT TERMINATION/CLOSEOUT SHEETDate 4/8/86Project No. E-26-675 or E-25-678School/~~XXX~~ ME/NEIncludes Subproject No.(s) N/AProject Director(s) Dr. Glen Bateman / W.M. Stacey ~~XXXX~~ GTRI / GITSponsor Department of Energy; Oak Ridge, TNTitle Saturated Tearing Modes in Tokamaks with DivertorsEffective Completion Date: 6/30/85 (Performance) _____ (Reports) _____

Grant/Contract Closeout Actions Remaining:

- ☒ None
- ☐ Final Invoice or Final Fiscal Report
- ☐ Closing Documents
- ☐ Final Report of Inventions
- ☐ Govt. Property Inventory & Related Certificate
- ☐ Classified Material Certificate
- ☐ Other _____

Continues Project No. _____ Continued by Project No. _____

COPIES TO:

Project Director
Research Administrative Network
Research Property Management
Accounting
Procurement/EES Supply Services
Research Security Services
Reports Section
Legal Services

Library
GTRI
Research Communications (2)
Project File
Other Heyser, Embrey, Jones

Saturated Tearing Modes in Tokamaks with Divertors

Contract No. - DE-AS05-81ER53117

Quarterly Progress Report

for April 1 - 30 June 1981

Prepared by

Professor Glenn Bateman
School of Nuclear Engineering
Georgia Institute of Technology
Atlanta, GA 30332

June 29, 1981

Saturated Tearing Modes in Tokamaks with Divertors

Contract No. - DE-AS05-81ER53117

Quarterly Progress Report

Finite Aspect Ratio Model

We have developed a finite aspect ratio self-consistent model for saturated tearing mode magnetic island widths in plane slab and cylindrical geometries. The key to the finite aspect ratio theory is the observation that there is a helical Pfirsch-Schlüter like charge separation driven by magnetic islands and the surrounding magnetic perturbation. This charge separation sets up a helically modulated electric field poloidally around the plasma. When this effect is included in the model, the parallel current density derived from the parallel component of Ohm's law can be made to satisfy the local equilibrium conditions throughout the magnetic island and surrounding perturbation. When the flattening of the current profile in the presence of the magnetic island is properly calculated using this procedure, the resonant singularity is removed from the ordinary differential equation for each harmonic of the radial magnetic field, and the island width (which acts like a generalized eigenvalue in the differential equation) can be determined using a straightforward computation. The perturbation expansion is based entirely on the width of the magnetic island relative to the plasma minor radius, independent of the aspect ratio. Note, it is found that the helical Pfirsch-Schlüter effect driven by saturated tearing modes vanishes in the large aspect ratio limit.

This development of a finite aspect ratio theory in simple geometry (plane slab, circular cylinder) opens up the way for studying the effect of a bundle divertor and ripple coils on magnetic islands -- since the helical harmonics of these localized perturbations depend on the aspect ratio. The

theory is also an essential link to the study of saturated tearing modes in toroidal geometry, where the plasma shift and toroidal deformation of the current profile are essentially finite aspect ratio effects.

Work is in progress to develop the model in arbitrary toroidal geometry using flux coordinates and the flux-surface averaged parallel component of Ohm's law. Essentially, the model presented by Shafranov and Zakharov ^(1,2) is being adapted to determine steady state magnetic island widths driven by saturated tearing modes, together with the helical component of applied magnetic fields, and consistent with reasonable profiles of parallel electrical conductivity and scalar pressure. A perturbation expansion using the width of the magnetic island relative to the plasma radius together with decomposition into helical harmonics will be used as necessary to implement the model.

Effect of Bundle Divertor and Ripple Reduction Coils

Along a second line of research in progress, we have set up an efficient field line following code, on the MFE computer, designed to study magnetic islands and similar magnetic structures resulting from the applied magnetic field of a bundle divertor ⁽³⁾, hybrid divertor ⁽⁴⁾, ripple reduction coil set ⁽⁵⁾, or similar coil set. It has been found, for example, that the ripple reduction poloidal field coils described in GTFR-26 ⁽⁵⁾ produce a plasma that has almost negligible departure from axisymmetry. Work is in progress to study the magnetic islands produced by (the vacuum magnetic of) a simple bundle divertor ⁽³⁾ compared to a hybrid bundle divertor ⁽⁴⁾ and compared to a hybrid bundle divertor which is tilted relative to the midplane. For example, the hybrid bundle divertor, with its long wing coils, can produce strong resonant field line excursions which may necessitate a reoptimization of the coil design. The field line

following code will also be used to study the effect of nonaxisymmetric bulges in the plasma current.

References

1. G. V. Perevergeev, V. D. Shafranov, L. E. Zakharov, "On the Evolution of Tokamak Plasma Equilibria," Third International Conf. on Plasma Theory (Kiev), Trieste, 1977.
2. L. E. Zakharov and V. D. Shafranov, "Problems in the Evolution of Equilibria of Toroidal Configurations," Kurchatov Institute Report IAE-3075 (1978) translated by J. T. Hogan, ORNL/TR-4667 (1980).
3. G. Bateman, P. Theriault, R. N. Morris, "Bundle Divertor Studies," Georgia Tech Fusion Report GTFR-20 (October, 1980).
4. G. Bateman and P. Theriault, "Hybrid Bundle Divertor Design," GTFR-23 (February, 1981).
5. G. Bateman, "Ripple Reduction Poloidal Field Coils for Tokamaks," GTFR-26 (March, 1981).

SATURATED TEARING MODES IN TOKAMAKS WITH DIVERTORS

Contract No. DE-AS05-81ER53117

Quarterly Progress Report
for 1 January - 31 March 1982

Prepared by

Professor Glenn Bateman
School of Nuclear Engineering and Health Physics
Georgia Institute of Technology
Atlanta, Georgia 30332

31 March 1982

SATURATED TEARING MODES IN TOKAMAKS WITH DIVERTORS

Contract No. DE-AS05-81ER53117
Quarterly Progress Report, March 29, 1982

by

Glenn Bateman
Georgia Institute of Technology

Saturated Tearing Modes in Toroidal Geometry

A formalism has been developed for the determination of saturated tearing mode amplitudes in axisymmetric toroidal geometry with no assumptions on the cross-sectional shape, aspect ratio, or plasma pressure (beta). The formalism entails an expansion of the 3D scalar-pressure plasma equilibrium equations to first order in the perturbed magnetic field--effectively an expansion in the width of the magnetic islands compared to the minor radius of the plasma. The problem encountered is that the perturbed current is best expressed in terms of the covariant components of the perturbed magnetic field, while $\nabla \cdot \mathbf{B} = 0$ is best expressed in the contravariant components. If flux coordinates are used and a Fourier decomposition taken in the angles, the relations between covariant and contravariant components produce Fourier convolutions under the derivatives and an intractable system of equations. The key to our formalism is to use the mix of contravariant and covariant components $(B^{1V}, B_\theta^1, B_\zeta^1, p^1)$ as the primary variables. A system of ordinary differential equations can then be derived for the helical harmonics $(B_{mn}^{1V}, B_{\theta mn}^1)$ as a function of V in Hamada coordinates (V, θ, ζ) . Fourier convolutions are needed only to evaluate the driving terms of these ordinary differential equations. The ODE's are formally singular at mode rational surfaces, but the presence of the magnetic islands will locally flatten the pressure and parallel resistivity profiles remove the singularity. The widths of the magnetic islands then serve effectively as eigenvalues for the solution of these ODE's as two-point boundary value problems. An iterative

algorithm can then be used to simultaneously adjust the widths of all the islands being considered, determine their effect on the axisymmetric profiles, solve for the adjusted axisymmetric equilibrium, solve the ODE's for the helical harmonics, and determine the new widths of the magnetic islands to close the cycle.

Computer codes have been obtained from S. C. Jardin, K. M. Ling and D. Monticello for the rapid computation of metric elements in Hamada coordinates for axisymmetric equilibria. These codes will be combined together with our code for the self-consistent determination of helical harmonics in toroidal geometry as soon as possible.

Effect of an Applied $7/4$ Mode on the $2/1$ Saturated Tearing Mode

The effect of an applied $7/4$ magnetic island on the amplitude of a $2/1$ saturated tearing mode was studied with a computer code which can self-consistently determine the amplitudes of several helical harmonics simultaneously in a circular cylinder. Starting with typical experimentally measured profiles, it was found that the $7/4$ islands are swallowed up by the $2/1$ islands and have no effect if the $2/1$ tearing mode is already at full amplitude before the $7/4$ mode is turned on. However, if the $7/4$ mode is applied before the $2/1$ has had a chance to grow, the local profile flattening at the $7/4$ mode rational surface can significantly suppress the saturated amplitude of the $2/1$ mode. Unfortunately, the combined widths of the $7/4$ and $2/1$ islands remain nearly constant over a wide range, and nearly equal to the width of the original $2/1$ saturated tearing mode. The combined widths, including the sawtooth region, are also nearly constant.

Effect of a Hybrid Bundle Divertor

When the vacuum magnetic field from a localized coil arrangement (e.g., from a bundle divertor) is superimposed on an axisymmetric plasma equilibrium, it is found that there is a threshold beyond which the perturbation produces complete lack of field line confinement outside of a given minor radius. Within the context of this model, we have found that the best available hybrid bundle divertor design at full current produces a lack of field line confinement over most of the plasma. Alternative hybrid bundle divertor designs are being considered in which the divertor coils are tilted or shortened to minimize the problem.

BACKGROUND

There is substantial evidence that large scale magnetic islands due to saturated tearing modes are responsible for the disruptive instability in tokamaks as well as for the observed Mirnov oscillations, soft x-ray signals and possibly enhanced transport as a function of the q-value⁽²⁻¹²⁾. It is known that an essential feature leading to the saturation of tearing modes is the local flattening of the longitudinal current profile due to the structure of the magnetic islands^(1,7,8). It is known that the saturation width depends sensitively on the current profile. With noncircular cross section and toroidicity, harmonic coupling also has a strong effect on saturated tearing mode island widths⁽⁹⁻¹²⁾.

Most of the theoretical models developed so far for saturated tearing modes are valid only in the limit of large aspect ratio and low beta⁽⁹⁻¹⁴⁾. The plasma distortion in a tokamak with finite aspect ratio, particularly at high beta, is a significant effect which is just beginning to be treated properly. Until recently there has been no way to predict magnetic island widths due to saturated tearing modes in proposed tokamak reactors such as FED/INTOR⁽¹⁵⁾ or in lower aspect ratio devices such as spheromaks. Yet the disruptive instability, which is apparently caused by the overlap of magnetic islands, has been a problem in all tokamak experiments operated to date.

WORK IN PROGRESS:

Saturated Tearing Modes in Toroidal Geometry

A formalism has been developed for the determination of saturated tearing mode amplitudes in axisymmetric toroidal geometry with no assumptions on the cross-sectional shape, aspect ratio, or plasma pressure (beta). The formalism entails an expansion of the 3D scalar-pressure plasma equilibrium equations to first order in the perturbed magnetic field--effectively an expansion in the width of the magnetic islands compared to the minor radius of the plasma. The problem encountered is that the perturbed current is best expressed in terms of the covariant components of the perturbed magnetic field, while $\nabla \cdot \mathbf{B} = 0$ is best expressed in the contravariant components. If flux coordinates are used and a

Fourier decomposition taken in the angles, the relations between covariant and contravariant components produce Fourier convolutions under the derivatives and an intractable system of equations. The key to our formalism is to use the mix of contravariant and covariant components (B^{1V} , B_θ^1 , B_η^1 , p^1) as the primary variables. A system of ordinary differential equations can then be derived for the helical harmonics B_{mn}^{1V} , B_{mn}^1) as a function of V in Hamada coordinates (V, θ, η) . Fourier convolutions are needed only to evaluate the driving terms of these ordinary differential equations. The ODE's are formally singular at mode rational surfaces, but the presence of the magnetic islands locally flattens the pressure and parallel resistivity profiles and consequently removes the singularity. The widths of the magnetic islands then serve effectively as eigenvalues for the solution of these ODE's as two-point boundary value problems. An iterative algorithm can then be used to simultaneously adjust the widths of all the islands being considered, determine their effect on the axisymmetric profiles, solve for the adjusted axisymmetric equilibrium, solve the ODE's for the helical harmonics, and determine the new widths of the magnetic islands to close the cycle.

This algorithm is now being implemented in the form of a computer code. This code has evolved in the following steps:

- 1) It was decided first to write the part of the code which determined the axisymmetric equilibrium in Hamada coordinates given profiles with suitable flat spots in the neighborhood of each of the magnetic islands being considered. After considering a variety of options, the variational method of solving the inverse Grad-Shafranov equation looked the most promising⁽¹⁶⁾. For various technical reasons, neither of the existing codes^(16,17) proved suitable for our needs. Consequently, a new code has been written, which is closely patterned after the ORNL VMOMS code⁽¹⁶⁾ wherever possible.
- 2) The Georgia Tech code uses an adaptive integrator to accurately determine the equilibrium at any flux surface given equilibrium profiles with any number of flat spots. The conversion to Hamada coordinates is then made in order to determine the coefficients needed in the perturbed field equations in such a way as to minimize aliasing errors and retain the accuracy needed.

- 3) We are now in the process of implementing the procedure which will solve the perturbed field equations as a two point boundary value problem using an iteration on the island widths. The logic of this procedure, including the possibility of island overlap and vanishingly small islands, for example, has already been worked out in considerable detail in our circular cylinder version of this algorithm.

Effect of an Applied $7/4$ Mode on the $2/1$ Saturated Tearing Mode in Circular Cylinder Geometry

The effect of an applied $7/4$ magnetic island on the amplitude of a $2/1$ saturated tearing mode was studied with a computer code which can self-consistently determine the amplitudes of several helical harmonics simultaneously in a circular cylinder. Starting with typical experimentally measured profiles, it was found that the $7/4$ islands are swallowed up by the $2/1$ islands and have no effect if the $2/1$ tearing mode is already at full amplitude before the $7/4$ mode is turned on. However, if the $7/4$ mode is applied before the $2/1$ has had a chance to grow, the local profile flattening at the $7/4$ mode rational surface can significantly suppress the saturated amplitude of the $2/1$ mode. Unfortunately, the combined widths of the $7/4$ and $2/1$ islands remain nearly constant over a wide range, and nearly equal to the width of the original $2/1$ saturated tearing mode. The combined widths, including the sawtooth region, are also nearly constant.

Effect of an Applied Helical Field on Marginally Stable Tearing Modes

The circular cylinder code was also used to check on an effect observed by Lee et al.⁽¹⁸⁾ We found that self-consistent magnetic island widths are at least 2 to 3 times wider than the vacuum island widths from an applied helical field for marginally stable profiles. As the applied field is increased, however, the island width asymptotically approaches the vacuum island width. The difference is only 25% to 30%, for example, when the applied field is large enough to make the observed island width equal to 0.06 times the minor radius.

Effect of a Hybrid Bundle Divertor

When the vacuum magnetic field from a localized coil arrangement (e.g., from a bundle divertor) is superimposed on an axisymmetric plasma equilibrium, it is found that there is a threshold beyond which the perturbation produces complete lack of field line confinement outside of a given minor radius. Within the context of this model, we have found that the best available hybrid bundle divertor design at full current produces a lack of field line confinement over most of the plasma. This observation, supported by other researchers, effectively kills the hybrid bundle divertor as a viable option for tokamak reactors at this time.

PROPOSED WORK

During the next contract year we propose to:

- 1) Complete, refine, document and publish our computer code which is designed to determine multiple saturated tearing mode magnetic island widths in toroidal plasmas with low aspect ratio, noncircular cross section, and finite beta.
- 2) Carry out a survey in which we will vary the current profile, aspect ratio, cross-sectional shape, and pressure profile in order to determine the effect of these parameters on saturated tearing mode magnetic island widths.
- 3) Determine the effect of a selection of externally applied magnetic perturbation helical harmonics on these island widths.

While carrying out the above survey, particular attention will be paid to elucidating the physics of the coupling between different helical harmonics, the effect of multiple magnetic islands on the various plasma profiles (e.g. pressure and current profiles), and the potential of magnetic island overlap leading to a disruptive instability.

Our computer code is being designed in such a way that it could be later included as a module in a larger transport or equilibrium code.

BACKGROUND

Magnetic islands generated spontaneously by tearing modes and enhanced by externally applied magnetic perturbations are believed to be responsible for the disruptive instability and for some loss of plasma confinement in tokamaks [1-8]. Most of the research on saturated tearing modes has made use of large aspect ratio approximations to the toroidal plasma [7-10]. By developing a self-consistent method for treating nonlinearly saturated tearing modes in toroidal geometry with no approximation on the aspect ratio, cross sectional shape or beta [2,3], we have provided a means to study tearing modes in very low aspect ratio devices, such as JET or spheromaks, and in high beta tokamaks, such as most planned tokamak reactors and the Princeton Bean Experiment.

WORK IN PROGRESS:

During this last year we have had three achievements:

- 1) We have completed a computer code implementing our method for determining saturated tearing mode magnetic island widths in axisymmetric toroidal plasmas.
- 2) We have surveyed the effect of current profile, aspect ratio and plasma elongation on saturated tearing modes. Current peaking or suppression within the magnetic island is found to have a particularly large effect on the width of tearing mode islands.
- 3) A direct method has been found to compute Hamada coordinates from harmonics of the inverse Grad-Shafranov equation and a computer code based on this new method has been written.

Computation of Magnetic Islands in Toroidal Geometry

In April 1982 [3], we developed a self-consistent formalism for the determination of induced and spontaneous magnetic island widths in axisymmetric toroidal plasmas. This method makes no assumption on the plasma cross-section, aspect ratio, or beta. The only expansion parameter is the magnetic island width divided by the plasma radius. Since the effect of the magnetic islands on the background current profile is treated explicitly, any number of helical harmonics can be considered simultaneously. Harmonics

couple directly through the geometry of the equilibrium as well as indirectly through their effect on the background current profile. Using Hamada coordinates [1], the problem is reduced to solving a coupled system of ordinary differential equations for the covariant and contravariant components of the perturbed magnetic field helical harmonics.

This year, we completed a computer code GTDR [2] which implements this formalism. The equilibrium is computed using the variational moments method [11] to solve the inverse Grad-Shafranov equation. This method is fast enough to iterate 50 times or more while the island widths are varied to find a consistent perturbed solution. Adaptive predictor-corrector ordinary differential equation solvers are used throughout in order to achieve the high level of accuracy needed along the radial coordinate.

An important technical development, which substantially improved both the toroidal and cylindrical versions of the saturated tearing mode code, was to prescribe the slopes of the background profiles as functions of q as well as the radial coordinate. In particular, the local effect of the magnetic islands on the slopes of these profiles is expressed as a function of q while the global nature of the profiles is given as any prescribed function of the radial coordinate or poloidal flux. In this way, the flat spots produced by the magnetic islands are automatically self-centering and can be computed precisely, no matter how small the islands are.

The GTDR code is internally well organized and well documented [2]. External documentation has been written for a major part of it, and the rest is in preparation. In the large aspect ratio limit, island widths have been found to agree to better than two significant figures of accuracy with a cylindrical saturated tearing mode code, with no adjustment needed. GTDR typically needs two minutes of CRAY cpu time to iterate from a poor initial guess for one harmonic, eight minutes for two harmonics. Results are smooth and consistent.

Parameter Surveys

The parameter survey results summarized below will be reported in more detail in the PhD thesis of R. N. Morris [2] and in subsequent publications during the forthcoming year. Wherever possible, results obtained from the toroidal saturated tearing mode code GTOR were corroborated with the much simpler cylindrical code. Agreement in the large aspect ratio limit has been excellent.

The slope of the current profile in the neighborhood of the mode rational surface seems to have the strongest effect on the width of spontaneously occurring saturated tearing mode magnetic islands. Large changes of island width can be effected by making relatively modest changes in the slope of the current profile just off the inner shoulder of the magnetic island, in particular, while holding the slope of the rest of the profile fixed. These localized changes in slope have little effect on the global appearance of the profile. Stable tearing modes can be destabilized by making local changes in the slope of the current profile near the appropriate mode rational surfaces. We find that the natural asymmetry of the islands along the minor radial coordinate has only a modest 10% effect on the width of the tearing modes. If the conducting wall is distant from the edge of the plasma, profiles that place a given tearing mode near the edge of the plasma produce wider magnetic islands than profiles that place the tearing mode closer to the center of the plasma. The presence of a wider region of central current profile flattening due to sawtooth oscillations, or the presence of a $3/2$ magnetic island, which is closer to the center of the plasma than the generally more unstable $2/1$ island, has the effect of steepening the current profile and thereby producing a wider $2/1$ island.

Current peaking inside an existing tearing mode magnetic island has a striking effect on the nonlinearly saturated width of that island. Modest current peaking, which may be caused by Ohmic or other heating within the island, can increase the width of the island by factors of two or more. Conversely, a modest suppression of the current within the magnetic island, which may be caused by radiative losses within an island being heated primarily by conduction from the hot central core of the plasma, is observed to reduce or even completely extinguish saturated tearing modes. The implication is that the island width depends sensitively on details of the current profile that are so localized and, in some cases, so small that they are difficult or impossible to observe or infer from experimental evidence.

The effect of toroidicity and modest elongation of the plasma cross section has so far been observed to have a smaller effect than that of changes in the current profile. Force free toroidal plasmas with aspect ratios as low as 1.5 have been considered to date. If the current profile is held fixed, reducing the aspect ratio has the effect of moderately reducing the width of the tearing mode islands, for the profiles considered so far. The effect of harmonic coupling, in which a naturally unstable $2/1$ island drives a $3/1$ island (which would otherwise be stable), has been observed in plasma equilibria with elongated cross section.

Direct Computation of Hamada Coordinates

A direct method has been developed for the determination of Hamada coordinates [1] by solution of the inverse Grad-Shafranov equation given the source functions $p'(\psi)$ and $FF'(\psi)$, and given the shape of the outer boundary of the plasma. This work was carried out with Dr. R. G. Storer at the Flinders University of South Australia, supported by the South Australian government. A version of the computer program written in Australia has been installed and documented on the MFE C machine, and further refinements were made under the support of this USDOE contract [12].

This development has direct bearing on our saturated tearing mode research, since we need to recompute the background axisymmetric equilibrium during each iteration of the magnetic island width in the GTOR code. At present, the variational moments method followed by a mapping to Hamada coordinates is used in the GTOR code. Unfortunately, using this procedure, the resulting metric elements are then functions of the coordinates found by the moments method - not of Hamada coordinates. Further integrations over these extraneous coordinates must then be carried out during the computation of mode mixing terms for the tearing modes. When the new direct method for the determination of Hamada coordinates is implemented in the GTOR code, the result should be a cleaner and much faster calculation.

In the newly developed method, the problem of determining Hamada coordinates is reduced to the solution of a system of ordinary differential equations for the poloidal harmonics of the inverse Grad-Shafranov equation together with the equation for the Jacobian. A high degree of accuracy is achieved by using an adaptive predictor-corrector ODE solver. Agreement to four significant figures has been achieved using six poloidal harmonics in a comparison with the Solov'ev equilibrium [1] with aspect ratio 3. Special boundary conditions must be used at the magnetic axis, and the equations must be integrated from the magnetic axis out, in order to avoid a weak logarithmic singularity at the magnetic axis. Each integration of the equations out to any flux surface in the plasma yields a valid equilibrium, which can be used as is, in less than a second of CRAY cpu time. Alternatively, parameters can be varied at the magnetic axis in order to match the outer boundary of the plasma to any prescribed shape.

PROPOSED WORK

During the next contract year we propose to do the following research:

- 1) Couple one of the Georgia Tech saturated tearing mode codes to an existing transport code in order to study the effects of magnetic islands on global transport as well as the effects of transport-driven current profiles on saturated tearing mode magnetic island widths.

Doug Post and his group at Princeton have expressed an interest in including the effect of magnetic islands in the BALDUR code. It would probably be best to start with one of our simpler tearing mode codes in circular cylinder geometry before proceeding on to the full toroidal version. One of the problems to be resolved is how to incorporate the local flattening of the current and pressure profiles, dictated by the presence of each magnetic island, within the context of transport-driven profiles. The effect of current peaking or suppression due to heating or cooling within magnetic islands, which has a large effect on the width of saturated tearing modes, will be studied in a consistent manner.

- 2) Substantially improve the GTOR code by including the effect of the $m=1$ mode and by incorporating the newly developed direct method for the determination of Hamada coordinates together with an improved iteration scheme. The objective will be to include more helical harmonics in the computation of saturated tearing modes for high beta, elongated, and bean shaped toroidal plasma equilibria. It is hoped that between 10 and 100 helical harmonics will be feasible, with modest computational times.
- 3) If funds are available, a method for determining the amplitude of the helical harmonics in Hamada coordinates resulting from prescribed external coil currents will also be developed. The GTOR code, in its present form, can self-consistently compute magnetic island widths once the amplitudes of any resonant applied helical harmonics are known in terms of Hamada coordinates at the edge of the plasma.

A SURVEY OF THE METHODS
OF MHD ANALYSIS OF
MAGNETIC ISLANDS

by

R. N. Morris
Georgia Institute of Technology
Atlanta, GA 30332

November 1983

ABSTRACT: This work explains the structure, the importance of, and the MHD analysis of tearing modes. The reduced MHD equations are shown to offer the ability to follow the time evolution of tearing modes, but at a high cost in computer resources. The quasilinear equations are shown to have the ability to model more complex geometric situations, but at the expense of the time dependence of the equations. The derivation of both methods are outlined.

1. A QUALITATIVE OUTLINE

Magnetic islands belong to a class of perturbations known as internal modes which are believed to exist in controlled fusion devices such as tokamaks and stellarators. Internal modes differ from other types of perturbations in that their major effects are in the internal rather than boundary or edge regions of the plasma. These effects may manifest themselves as topological changes to the plasma proper and may radically alter the plasma confinement and its global stability. Their major impact is to alter the internal magnetic field configuration which:

1. Causes enhanced transport of plasma particles and energy due to the destruction of closed magnetic surfaces;
2. Produces Mirnov oscillations by the torodial rotation of the saturated instability (tearing mode);
3. Causes, in the most pathological cases, the major disruption when two tearing modes of different helicity overlap.

Magnetic islands are resonance phenomena - that is, a relatively small perturbation can have its effect enhanced by resonating, or strongly interacting in very specific regions of the plasma. Specifically, these regions are those closed magnetic field lines or rational flux surfaces. (A closed magnetic field line is a magnetic field line that closes on itself after traversing around the torus an integer number of times [1-12].)

The spontaneously growing perturbations which cause magnetic islands are known as tearing modes, since they cause the magnetic field lines to "tear" or break and reconnect to form a new and different magnetic configuration. Magnetic islands can also be induced by externally applied nonaxisymmetric magnetic perturbations and by other related instabilities. These mechanisms are beyond the scope of this paper.

Magnetic islands are major topological deviations from the simple nested flux surface model for MHD equilibrium [1,2,40]. Rather than the magnetic surfaces being composed of concentric tori as shown in Figure 1-1, an equilibrium with magnetic islands has helically distorted cylinders within the

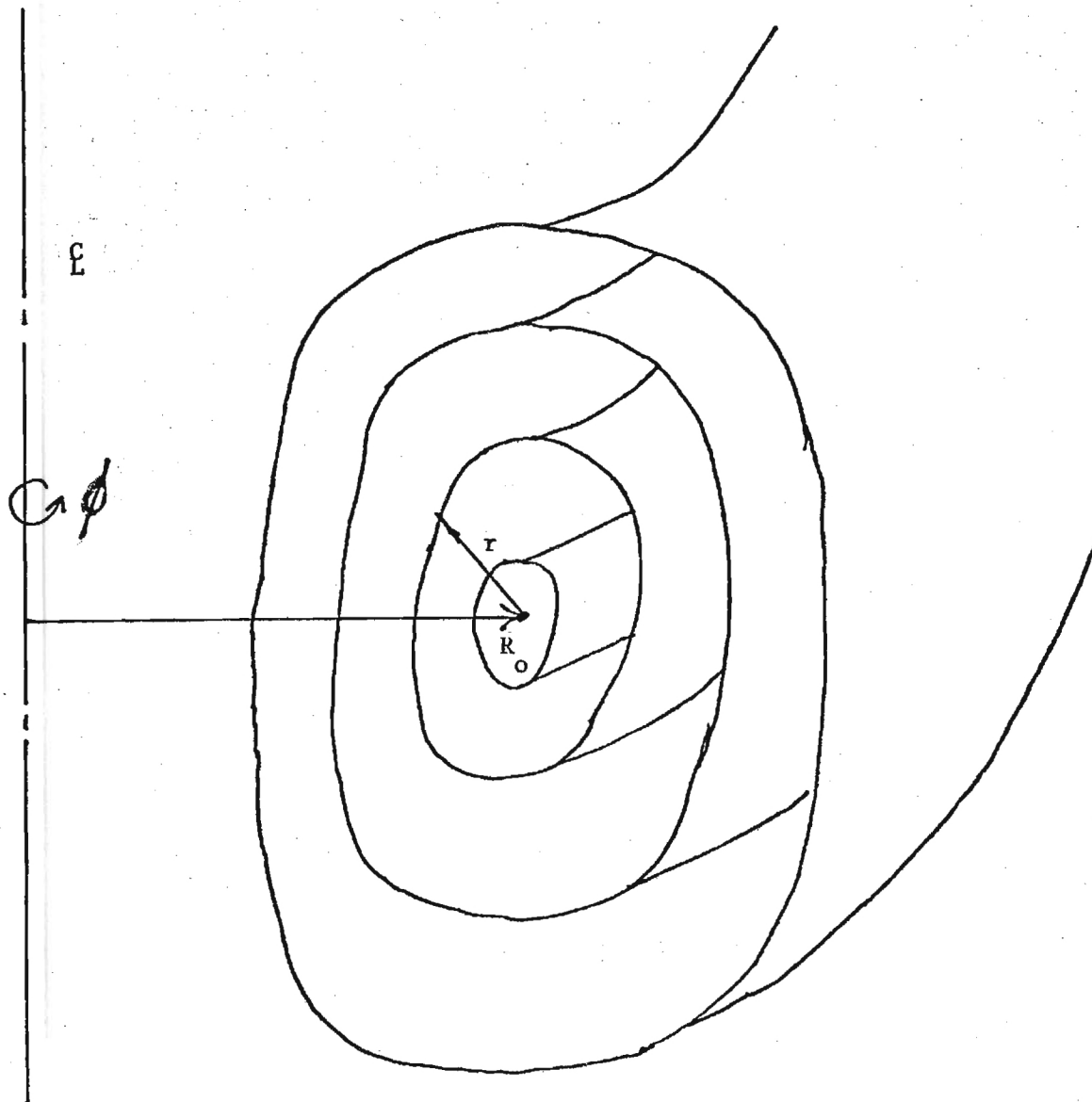


Figure 1-1. Simple nested flux surfaces
in an MHD equilibrium.

simply nested tori as well (see Figure 1-2). The nucleus of each magnetic island is a closed magnetic field line which supports a resonant perturbation (for a qualitative description and an example see Appendix A). Unlike other types of magnetic perturbations, the tearing mode is capable of large scale effects on the plasma even though the amplitude of the mode itself is many times smaller than the other equilibrium quantities. It is the fact that the background equilibrium can be and is effected by the tearing mode that generates the difficulty and the interest in studying the phenomenon [1,12,13,14,15].

The two important parameters that characterize an island are its helicity number and its width. The helicity numbers, which are the m and n numbers (i.e. 2/1, 3/1/ etc.), indicate the island location and with that magnetic surface its interacts. The relationship between the m and n number is

$$nq - m = 0 \quad (1)$$

where q is defined as the limit of the ratio of the number of turns a magnetic field line makes as it travels the long way around the toroid divided by the number of turns it makes as it travels the short way around. M is the periodicity in the poloidal angle, while n is the periodicity in the torodial angle.

The width of the island is defined as the maximum radial width across the island region. It is approximately

$$w = 4 \left(\frac{B_{mn}^{1v}}{n B^{0\theta} \frac{dq}{dv}} \right)^{1/2} \quad (2)$$

where all quantities are evaluated at the mode rational surface. B_{mn}^{1v} is the perturbed radial field, q is the inverse rotational transform, and $B^{0\theta}$ is the poloidal field (see Appendix D). This formula has been tested in various computer experiments and found to be in good agreement [11,12].

Magnetic islands are observed to rotate in the toroidal direction, in the direction of the electron drift resulting from the plasma current. This paper will not address this rotation, but rather will assume its existence as it does not enter into the MHD analysis [19].

The most serious problem speculated to be caused by magnetic islands is the major disruption.[16,17, 18,19]. Major disruptions can be classified in two ways: a hard disruption in which the entire plasma is dumped out on a microsecond to hundreds of microseconds time scale and a soft disruption in which the plasma confinement decreases suddenly, but not to a point from which recovery is impossible [16,21]. The mechanism for the hard disruption is thought to be the overlap of two

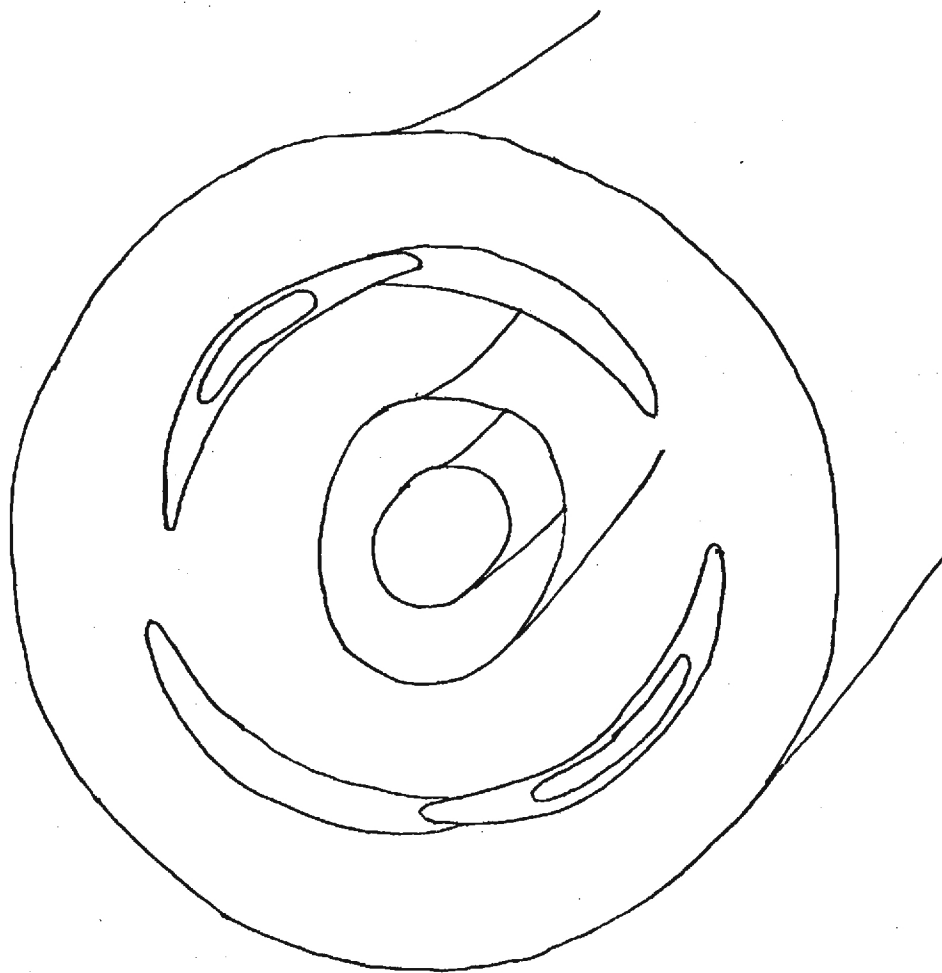


Figure I-2

islands which generates a large stochastic magnetic region within the plasma volume destroying the plasma confinement. The soft disruption is a more benign effect, in which an island may interact with the plasma interior and the wall limiter providing a transport short circuit, which may or may not be fatal to the discharge [16,17, 18-28].

Magnetic islands, when uncoupled or only loosely coupled to each other, grow on a time scale of milliseconds. This growth rate is too slow to explain the sudden nature of the hard disruption which happens on a microsecond time scale. If, however, two magnetic islands of different helicity were to grow and overlap, the resulting region engulfed by the islands may explosively grow into a stochastic magnetic region of poor confinement and, if the initial islands were large enough, a large percentage of the plasma confinement would be destroyed thus terminating the discharge. The most probable causes for the major or "hard" disruption are either the overlapping of the $m=2$, $n=1$ island with the $m=3$, $n=2$ island and the lack of confinement due to the large stochastic region thus generated, or a combination effect in a high density plasma where the $2/1$ island overlaps both the $3/2$ island and the limiter. This occurrence destroys the plasma confinement by introducing a large thermal loss and an influx of impurities to the plasma interior. The soft disruption may be the result of a single island connecting the internal plasma volume with the limiter. This will transfer large quantities of plasma energy out of the main plasma volume, but if the island disappears soon enough recovery may be possible. The $2/1$ island seems to be the dominant island in this case [16].

Unlike disruptions, Mirnov oscillations are a relatively mild instability [2,3,29,30,31]. They manifest themselves as small oscillating helical perturbations in the poloidal magnetic field. These perturbations usually settle down to a saturated level as the discharge becomes established and have an oscillation frequency in the neighborhood of 10kHz. This oscillation is believed to be caused by the toroidal rotation of the tearing modes at the electron diamagnetic drift velocity. As the Mirnov oscillations increase in amplitude the energy confinement time of the plasma drops and the sudden disappearance of the oscillations may be a precursor to a major disruption.

The other major concern is the effect of magnetic islands on transport. Since the islands have a width, they provide a transport short circuit which may be responsible for enhanced transport [1,2,3]. One example of this is the flattening of the temperature and the density profiles in the plasma interior caused by sawtooth

oscillations. These oscillations are caused by a low mode number magnetic island ($n=1, m=1$) which periodically dumps plasma particles out of the center of the plasma and into neighboring regions. To analyze this low mode number island requires the inclusion of inertial terms which will not be addressed by this paper [3,29,30,31]. The islands may also enhance particle loss of fast and trapped particles. The situation becomes even more complex when islands of different helicity overlap and produce a stochastic field region. This will presumably result in a region with no confinement since the particles will traverse this region on a time scale of the thermal velocities, rather than the diffusion time scale [3,11,18]. Electrons may be effected to a much greater degree than ions, since they have a much smaller gyro radius which allows them to respond the spatially finer scale perturbations [32].

That an equilibrium with islands is possible is founded on two ideas:

1. A magnetic island can be a lower magnetic energy configuration; and
2. The existence proofs for some series solutions of n body problems shown by Kolmogorov, Arnold, and Moser. (KAM).

As will be described later, magnetic islands allow for local flattening of the current profile which effectively lowers the energy stored in the poloidal field. This is consistent with the observed voltage spike seen at the onset of a disruption. The inductance of the plasma is:

$$L = \frac{1}{I^2 \mu_0} \int_V \vec{B} \cdot \vec{B} \, dv \quad (3)$$

where L is the inductance, I is the total current and B is the magnetic field. It can be shown that a broader current density profile can have a somewhat lower inductance than one with a steeper profile. (See the chapter on quasilinear analysis). In later sections it will be shown that the steeper current profile may provide a driving force to produce the island.

The voltage around the torus is

$$V = IR + \frac{d}{dt}(LI) \quad (4)$$

where V is the voltage and R is the plasma resistance. If a magnetic island were to suddenly grow, or more importantly two islands were to overlap, the inductance

of the plasma would decrease due to the resultant current flattening. The $\frac{d}{dt}(LI)$ term would be large if this happened on a short time scale (island overlap). Since I is generally held constant in tokamak experiments:

$$\frac{d}{dt}(LI) = I \frac{d}{dt} L \quad (5)$$

Since L decreases in time (due to the changing current profile) $\frac{dL}{dt}$ is negative and the disruption manifests itself as a negative voltage spike at the transformer [19].

The KAM proof demonstrated, in the context of classical physics, that it was possible to have a perturbation that destroyed some tori of phase space, but left the others intact (though distorted) [33,34,35,36]. It was this idea that led to the belief that it was possible for a magnetic field to take on these characteristics. It is found that the low-order resonances produce the widest islands and thus are to a first approximation the most important [33,34].

This connection may be examined by the correspondence between field line trajectories and the orbits of a hamiltonian system [11,37,38]. Choosing the simple case of a magnetic field with cylindrical symmetry, the hamiltonian may be shown to be

$$H + H_0(v) = \int_0^r B_\theta / r \, dr \quad (6)$$

with $V = \int_0^r k B_\phi \, dr$

Using Hamilton's equations:

$$\dot{\theta} = \frac{\partial H}{\partial v}; \quad v = \frac{-\partial H}{\partial \theta} + \frac{\partial V}{\partial \phi}$$

it can be shown that the magnetic field line trajectory is:

$$\theta = w\phi + \theta(0)$$

where $w = \frac{1}{q(v)}$

v, θ, ϕ are coordinates on a phase space tori: v is a radial coordinate, θ a poloidal angle, and ϕ is a toroidal angle. B_ϕ, B_θ are the magnetic field components in cylindrical geometry, k is the inverse of the major radius, and q is the inverse of the rotational transform.

The tearing mode may be represented as a perturbation to this hamiltonian:

$$H = H_0(v) + \delta\lambda(v)\cos(m\theta - n\phi) \quad (7)$$

where

$$\delta \ll 1$$

To analyze this equation it is first necessary to make a canonical transformation from v, θ, ϕ space to I, ξ, ϕ space with the generating function:

$$G(I, \xi, \phi) = -(v - v_s)(\xi + n\phi)/m \quad (8)$$

Giving for the connection between the old and new coordinates:

$$\theta = -\frac{\partial G}{\partial v} = (\xi + n\phi)/m \quad (9)$$

$$v = -\frac{\partial G}{\partial \xi} = (v - v_s)/m \quad (10)$$

The new hamiltonian is

$$H_N = H + \frac{\partial G}{\partial \phi} = H - (n/m)(v/v_s) \quad (11)$$

The region of interest is the region near $I_s = I(v_s)$; with $x = (I - I_s)$ expand (11) as:

$$H_N = H_0(I_s) + H'_0(I_s)x + H''_0(I_s)\frac{x^2}{2} - \frac{n}{m} + \delta\lambda(I_s)\cos\xi \quad (12)$$

The case of interest is where $H'_0 = n/m$. At that point the perturbation is in resonance with a closed orbit trajectory giving:

$$H_N = H_0(I_s) + \frac{H''_0(I_s)x^2}{2} + \delta\lambda(I_s)\cos\xi \quad (13)$$

Since the linear term has vanished, the particle now is trapped in a region of a different topological shape - a distorted helical cylinder within the phase space tori. The width of the radial displacement of the orbit can be found by equating the value of the hamiltonian at the x point of the separatrix with that at the edge

of the "Island". (Appendix D illustrates how this is done.) With separatrix at 0 and the widest part of the island at π , it can be shown that:

$$W = 4 \left(\frac{\delta \lambda(I)}{H_o} \right)^{1/2} \quad (14)$$

for the width.

To compare this to equation (2) use the following analogues:

$$q = \frac{1}{\frac{dH}{dv}} = \frac{m}{\frac{dH}{dI}} = \frac{m}{n} = \frac{B_o^2}{B}$$

$$H_o = - \frac{m^2}{2} \frac{dq}{dv} = -n^2 \frac{dq}{dv}$$

$$\lambda = \frac{-n B_o^2}{B}$$

Using these equations equation (2) can be reproduced from equation (14).

This completes the background introduction of simple magnetic islands. Other topics include the effects of multiple islands on each other, the effects of islands on the background equilibrium, and the overlap of magnetic islands with the generation of stochastic or chaotic magnetic field regions. The following chapters will outline the various methods used in the solution of the tearing mode equations.

2. PLANE SLAB ANALYSIS OF TEARING MODES

The simplest examination of tearing modes can be seen with the plane slab model in a cartesian coordinate system. Figure 2-1 $B_x(y)$ and $B_z(y)$ form the background equilibrium; b_y represents the perturbed magnetic field component of interest. (Note that this component is perpendicular to the background fields.) It is this component which forces the magnetic field line reconnection. The study of the plane slab model is useful even though it does not correspond to an actual experimental device, since it contains the fundamental physics without the complicated geometric terms [11,39,40]. The major shortcoming is that the effect of geometric mode coupling, which is present in the toroidal device geometry, is not present in this model and thus one of the more pathological aspects of this perturbation is omitted [3,18].

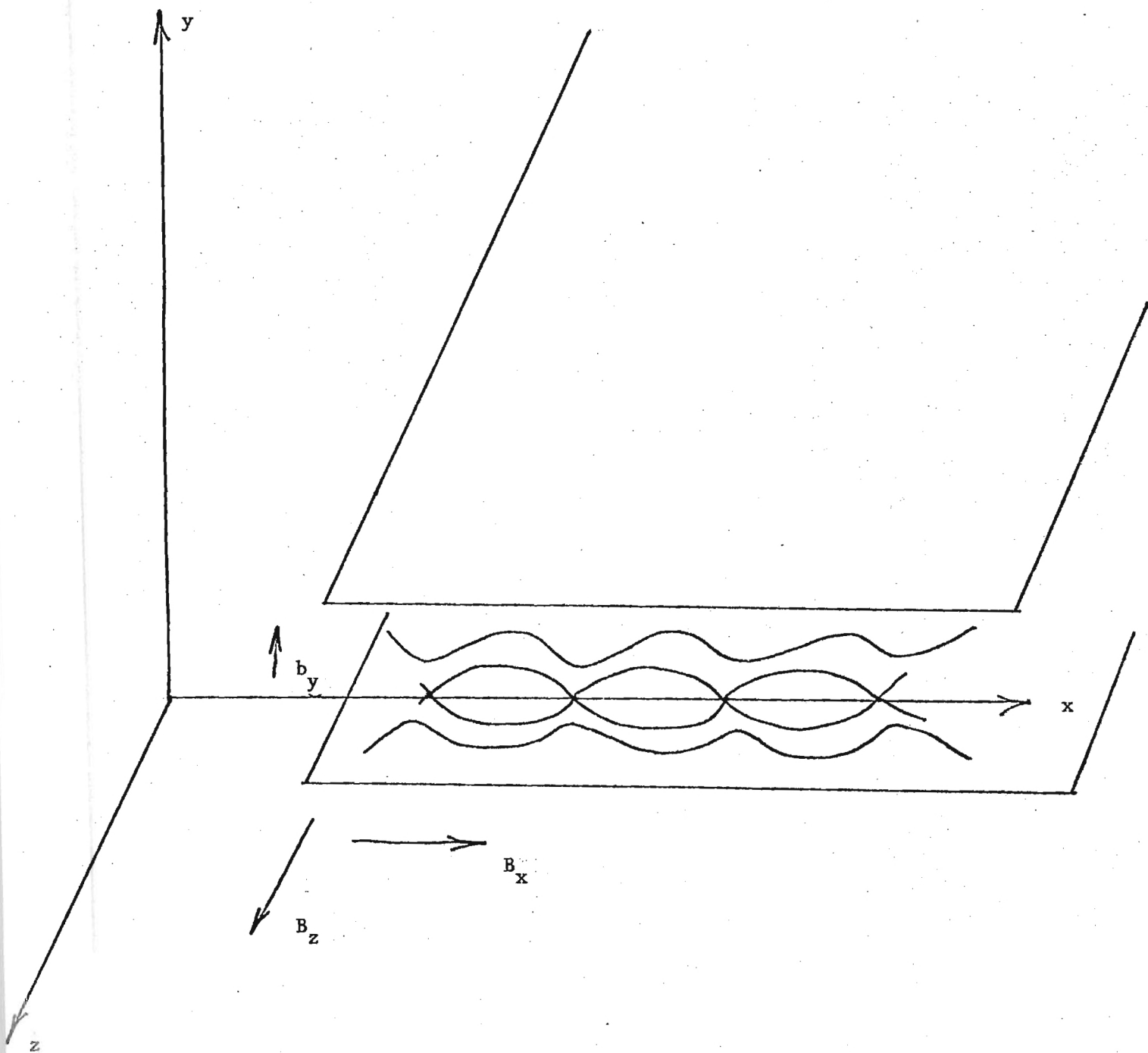


Figure 2-1. Magnetic Islands in a plane slab geometry.

The derivation of the plane slab equations requires the ideal MHD equations along with Ohm's Law for a plasma. Before this derivation is outlined, it is useful to examine the magnetic diffusion equation. To obtain it insert Ohm's Law:

$$\frac{\vec{J}}{\sigma} - \vec{v} \times \vec{B} = \vec{E} \quad (15)$$

into Maxwell's equation for the time rate of change of a magnetic field:

$$\nabla \times \vec{E} = -\frac{\partial \vec{B}}{\partial t} \quad (16)$$

Now use Ampere's law:

$$\mu_0 \vec{J} = \nabla \times \vec{B} \quad (17)$$

along with (15) and (16) to produce:

$$\nabla \times \left[\frac{\nabla \times \vec{B}}{\mu_0 \sigma} \right] - \nabla \times (\vec{v} \times \vec{B}) = -\frac{\partial \vec{B}}{\partial t} \quad (18)$$

where σ is the conductivity of the plasma, μ_0 is the permeativity of the free space, \vec{v} is the fluid velocity, and \vec{E} is the electric field. If σ is approximately constant the magnetic diffusion equation is produced:

$$\frac{1}{\mu_0 \sigma} \nabla^2 \vec{B} + \nabla \times (\vec{v} \times \vec{B}) = \frac{\partial \vec{B}}{\partial t} \quad (19)$$

The $\nabla^2 \vec{B}$ term allows magnetic lines of force to diffuse; that is, the topology of the magnetic surface can change over a time interval in contrast to the frozen field line model [11,39,40]. This is the important effect of resistivity - even very little resistance allows the magnetic field configuration to change or evolve in time. Consider the case where \vec{v} is small and can be neglected; then (19) becomes:

$$\frac{1}{\mu_0 \sigma} \nabla^2 \vec{B} = \frac{\partial \vec{B}}{\partial t} \quad (20)$$

If $\frac{\partial \vec{B}}{\partial t}$ is positive the field diffusion can grow and the tearing instability will develop. The particular case of interest (for this paper) is where $\frac{\partial \vec{B}}{\partial t}$ goes to zero since this represents a saturated island. (Neglecting the island rotation - a Finite Larmor Radius effect).

The MHD equations and Ohm's Law along with several simplifying approximations yield the following equations for b_y (See Appendix B).

Far from the rational surface the tearing mode equation is:

$$b_y'' - (k^2 + \frac{F''}{F})b_y'' = 0 \quad (21)$$

A rational surface is the surface at which the perturbation resonates. In this case the rational surface is located at $y = 0$.

Near the rational surface the equation must be rescaled and it becomes

$$b_y^V - (1 + \beta^2 w^2)b_y''' - 4\beta^2 w b_y = 0 \quad (22)$$

The variables are:

k = the wave number of the perturbation

$F = \vec{k} \cdot \vec{B}$

$\beta = \delta^2 F'(0)^2 / \mu_0 \rho \gamma^2$

$\delta^2 = 1 / \mu_0 \gamma \sigma$

γ = linear growth rate

ρ = fluid density

$w = y/\delta$

Because of the rescaling (22) is known as a boundary layer equation. This comes about because the derivatives of b_y , while small outside the resonance region, are no longer small (when compared to the equilibrium terms) within the resonance region. The rescaling effectively reorders the equation to handle this apparent break down in the ordering [41]. To produce an overall solution for b_y the plasma is divided into two regions - an outer region where the boundary layer solutions have no effect and an inner region where the solution is dominated by the boundary layer solution. Equation (21) is solved in the outer region starting at $y = + -a$

and extended to within $\pm \alpha$ of $y = 0$. (α is of the order of the resistive layer width). Within the region $\pm \alpha$ equation (22) is solved and matched to the outer solution from equation (21), thus forming a complete solution over the plasma. The reader is referred to Appendix B and to the references for the details.

One very important point is that b'_y is not small compared to the equilibrium quantities at the rational surface (hence the boundary layer equation). Since $\alpha \ll a$, b'_y , which shows up in $\nabla \times \vec{B}$, implies a sheet like current (on the scale length of the equilibrium terms) at the rational surface. It is this current that provides the driving force to break and reconnect the field lines thus shifting the plasma across the magnetic field [50]. If equation (21) were such that the solution was nonsingular over the entire plasma, then the boundary layer region would not exist and the driving force would be zero; in other words the island would be stable.

It is useful to define the normalized jump in the first derivative (Equation 21, outer solution)

$$\Delta' = (b'_y(\alpha) - b'_y(-\alpha))/b_y(0) \quad (23)$$

This may be thought of as a measure of the discontinuity of the first derivative of the outer solution and may be considered to be a measure of the stability of the equilibrium to tearing modes [11,39,40]. This "jump" (or more correctly the boundary layer behavior) provides the island driving force. If Δ' is positive it implies a growing tearing mode; if negative, a shrinking one. Δ' tending toward zero is the saturated island case; it is of principle interest in the steady state case because Δ' equal to zero is the special case solution to (21) in which no singularities appear. This special case will be covered in greater detail in the section on the quasilinear analysis.

To examine the velocity behavior near the rational surface consider the velocity component responsible for the transport of plasma across field lines (see Appendix B):

$$v_y = \frac{-i}{F} \left[\gamma b_y + \frac{1}{\mu_0 \sigma} (k^2 b_y - b''_y) \right] \quad (24)$$

Near the edge of the island, but still in the tearing region, b_y^{\parallel} becomes small compared to γb_y and V_y may be approximated as

$$V_y = \frac{-i\gamma b_y}{F} \quad (25)$$

since k^2 is small. Physically equation (25) shows that plasma is being transported across field lines. If Δ' is positive, this velocity is outward and the island is growing; if negative, the velocity is inward and island is collapsing. Thus as the tearing mode grows the plasma "squeezes" across the magnetic field. As the mode begins to saturate Δ' tends toward zero and a new equilibrium is established. The effect of Δ' is therefore to force plasma across field lines to a new configuration. This can and does effect the background equilibrium. Thus b_y can have a zero order influence even though it is of first order.

The slab model provides insight into the nature of tearing modes and provides a base for a more sophisticated analysis that includes the effects of cylindrical and toroidal geometry. Also note that the above Δ' analysis is not the only solution method; the following chapters will outline other approaches that may be preferred to study the long term growth and saturation of tearing modes.

3. THE REDUCED MHD EQUATIONS

The set of equations used most commonly to study tearing modes is a modification of the ideal MHD equations. The major modification is the additional of resistivity to the MHD equations which allows the magnetic field to change in time and to develop tearing modes [11,18,40,42]. The set of equations is:

$$\rho \frac{d\vec{v}}{dt} = -\nabla p + \vec{J} \times \vec{B} \quad (26)$$

$$\vec{J} = \nabla \times \vec{B} / \mu_0 \quad (27)$$

$$\frac{\partial \vec{B}}{\partial t} = -\nabla \times \vec{E} \quad (28)$$

$$\vec{E} + \vec{v} \times \vec{B} = \eta \vec{J} \quad (29)$$

These equations are approximated for certain limiting situations and this set of approximated equations form what is known as the reduced MHD equations. Before proceeding with any further analysis it should be pointed out that the reduced equations consider only:

1. The vanishing pressure case
2. The limit of only toroidal current
3. The limit of constant toroidal field
4. Large aspect ratio

While it is apparent that the above form a rather stringent set of limits, much work and insight has been obtained from the reduced MHD equations. They are essentially the only time dependent set of MHD equations that form a tractable set for a systematic study. They are used most often in computational studies that attempt to examine the growth and the nonlinear coupling between different helicity tearing modes.

The derivation of the reduced MHD equations is centered around the definition of the flux function ψ . The ideal MHD equations and Ohm's law are combined to produce a set of equations for the time rate of change of ψ , and this set of equations is then advanced in time to observe the evolution of ψ . See Appendix C for a derivation of the reduced MHD equations.

In the toroidal limit the Reduced MHD equations are:

$$\frac{\partial \psi}{\partial t} + \vec{v}_\perp \cdot \nabla \psi = \eta R J_\zeta = -\frac{\partial \phi}{\partial \zeta} \quad (30)$$

$$\mu_0 J_\zeta = \nabla_\perp^2 \left(\frac{\psi}{R} \right) + \frac{\psi}{R^3} \quad (31)$$

$$\vec{v}_\perp = \frac{1}{B_\zeta} (\nabla \psi \times \hat{\zeta}) \quad (32)$$

$$\rho \left[\frac{\partial u}{\partial t} + \vec{v} \cdot \nabla u \right] = \frac{-(\nabla \psi \times \nabla J_\zeta) \cdot \hat{\zeta}}{R^2} - \frac{B_\zeta}{R^2} \frac{\partial J_\zeta}{\partial \zeta} + \frac{J_\perp \cdot \nabla B_\zeta}{R} + \frac{\hat{z}}{R^2} \cdot (\vec{J} \times \vec{B}) \quad (33)$$

with $u = (\nabla \times \frac{\vec{v}}{R}) \cdot \hat{\zeta}$

In the cylinder limit

$$\frac{\partial \psi}{\partial t} + \vec{v}_\perp \cdot \nabla \psi = \eta R J_\zeta - \frac{\partial \phi}{\partial \zeta} \quad (34)$$

$$\mu_0 J_\zeta = \nabla_\perp^2 \left(\frac{\psi}{R} \right) \quad (35)$$

$$\vec{v}_\perp = \frac{1}{B_\zeta} (\nabla \phi \times \hat{\zeta}) \quad (36)$$

$$\rho \left[\frac{\partial u}{\partial t} + \vec{v} \cdot \nabla u \right] = \frac{-(\nabla \psi \times \nabla J_\zeta) \cdot \hat{\zeta}}{R^2} - \frac{B_\zeta}{R^2} \frac{\partial J_\zeta}{\partial \zeta} \quad (37)$$

with $u = (\vec{v} \times \frac{\vec{v}}{R}) \cdot \hat{\zeta}$

The variables are defined as:

- ψ flux function
- \vec{A} vector potential
- ϕ electrostatic potential
- \vec{v} fluid velocity
- η resistivity
- \vec{E} electric field
- \vec{J} current density
- ρ mass density
- μ_0 permeativity of free space

The coordinate system is shown in Figure C-1.

Note that the toroidal equations have an extra term, due to the expansion in the aspect ratio, that can and does influence the behavior of the evolution of ψ .

At this point it should be emphasized that several different approaches are being applied to the study of tearing modes using the reduced MHD equations. These are:

1. A linearized model which contains a singularity at the rational surface (see slab derivation) and relies on a Δ' type of matching;
2. A helical flux model which is limited to a two dimensional formulation, but requires less computational effort;

3. A nonlinear model in which the background is allowed to change as the perturbation develops, thus allowing the perturbation to effect the background; and
4. A quasilinear model in which the background is modified to provide a solution to a linearized tearing mode equation.

The helical flux model is the simplest of these models and has been extensively studied [4,13,18,43,53]. A simple analytic equilibrium with tearing modes has also been found for a helical flux function [45]. The base model for the study of the helical flux function centers around a Δ' type of analysis as in the slab; however saturation effects have been included by using a quasilinear method in which the perturbation is allowed to feedback and influence the functional form for the current; that is, the current profile is modified by the presence of an island [13]. It is found that certain current profiles exhibit varying degrees of stability against the formation of tearing modes. The saturation of the resulting island is due to the island sampling different portions of the background equilibrium. This gives a decrease in the Δ' driving term which is most strongly modified by the effect of the island width on the functional form of the background current profile near the island. This saturation width is proportional to Δ' ; thus a case may be completely unstable and not saturate. The initial current and resistivity profiles are important; a rounded current profile was observed to have larger saturated islands than either a peaked current model, or a flat current model [13].

The important point made by the above quasilinear analysis is that a quasilinear or fully nonlinear model is very useful to compute saturated island widths since Δ' is strongly effected by the current functional form near the island.

The helical flux model, while useful for the study of one harmonic, cannot be used to examine the effects of islands of different helicity on the plasma. It is therefore necessary to use a less stringent form of the reduced MHD equations to address this area. Of particular interest is how the islands effect each other, both in terms of growth rate and saturation width. The dynamics of two islands overlapping and the resulting effect on the plasma is another phenomenon which generates research interest as well.

Solving the reduced MHD equations in cylindrical geometry, with a three dimensional equation set rather than a two dimensional set, allows one to observe the coupling between islands and the resultant effect on the current profile. It

has been observed that the $2/1$ tearing mode can destabilize the $3/2$ mode resulting in large increases in the growth rate of the $3/2$ mode and the resultant increase in the $3/2$ island width. This destabilizing effect also extends to other islands as well; one effect of this destabilization is to increase the total plasma region occupied by these islands. In fact, if a suitably large number of islands is included, the entire plasma region may be destroyed, from the center to the limiter [17,18,46,47].

It is generally found that the growth rate of the islands transforms from an exponential growth rate to an algebraic growth rate as the islands grow in width [50]. The nonlinear coupling may change this result in some cases, resulting in the sudden growth of a favored mode at a much accelerated rate. This may explain the very sudden nature of the major disruption [17,18,46].

The magnetic islands cause sharp deformation in the toroidal current profile near the island x points and this deformation of current becomes even more severe as the number of islands increase. This in fact may have a major coupling effect between islands, since the saturated width of the islands are sensitive to the current gradient near the island edge [13,46,48]. This severe current deformation eventually limits the computer runs, as numeric problems soon develop [17,18,46]. Again this points to the need for a nonlinear or quasilinear approach to the solution.

Toroidal coupling has a profound effect upon the magnetic islands; it introduces a linear coupling effect between neighboring islands. This coupling effect causes normally stable islands to be destabilized by their unstable neighbor. This may cause both islands to grow and is responsible for the generation of satellite islands. Since these satellite islands manifest themselves as an increase in the stochastic magnetic field region, it is clear that this effect is important even in the large aspect ratio approximation [17,46,47]. Mathematically this comes about from the off diagonal terms of the metric tensor relating the contravariant and covariant vector components of the equilibrium magnetic field. Unfortunately this effect is very difficult to handle and has been only formulated in the time independent case for small aspect ratios [14].

It is clear that both the nonlinear mode coupling and the geometric mode coupling (toroidal) greatly effect the growth and saturation of magnetic islands. It is this nature of tearing modes that puts the stringent conditions on the equations used to study magnetic islands; apparently higher order terms (toroidal geometry, current profile modifications) must be included to form a reasonable approximation to the physical case.

4. QUASILINEAR AND ENERGY MODELS

As was seen in the previous Chapters, certain approximations have been made to form tractable computation equation sets for the study of tearing modes. The quasilinear model attempts to include the effect of the island on the background equilibrium to remove the apparent singularity at the rational surface. This model in effect eliminates the boundary layer solution, since the Δ' term is now zero. This solution is the special case solution to equation (21) in Chapter 1. Note that this solution corresponds to the saturated island case; therefore, in general, the quasilinear equations cannot follow the time evolution of the tearing mode. They can, however, handle more complex geometric situations and are useful to find saturated tearing mode in these more physical situations [8,12,13,14,15,43,48].

The simplest of these models may be obtained by taking the asymptotic time limit of the reduced MHD equations [2]. (See Appendix C). This limit produces, in circular cylindrical geometry:

$$\frac{d}{dr} \left(r \frac{d}{dr} r B_r \right) - m^2 B_r + \frac{m r^2 \mu_0 \frac{dJ_{z0}}{dr}}{(n k r B_{z0} - m B_{\theta 0})} = 0 \quad (38)$$

The most obvious part of this equation is the fact that the equation is singular at the point where $(r k n B_{z0} - m B_{\theta 0}) = 0$. This singularity arises from the fact that this equation does not apply in the region near the singularity before a tearing mode saturates (see slab model). The basic idea of the quasilinear analysis is to allow the magnetic island to modify the background equilibrium as necessary to support a saturated tearing mode [12,13,4] (see Appendix D).

Also note that besides the singularity another problem is apparent - equation (38) is a boundary value problem with no adjustable parameters or eigenvalues; apparently there is no solution. If, however, the magnetic island is allowed to modify the background equilibrium through J_{z0} it is possible that B_r could be made to exist. The question remaining is what self consistent functional form should be chosen for J_{z0} .

Because the magnetic island connects inner and outer regions of the plasma together, these connected regions will have similar density and temperature distributions because of the high thermal and particle conductivity of the plasma

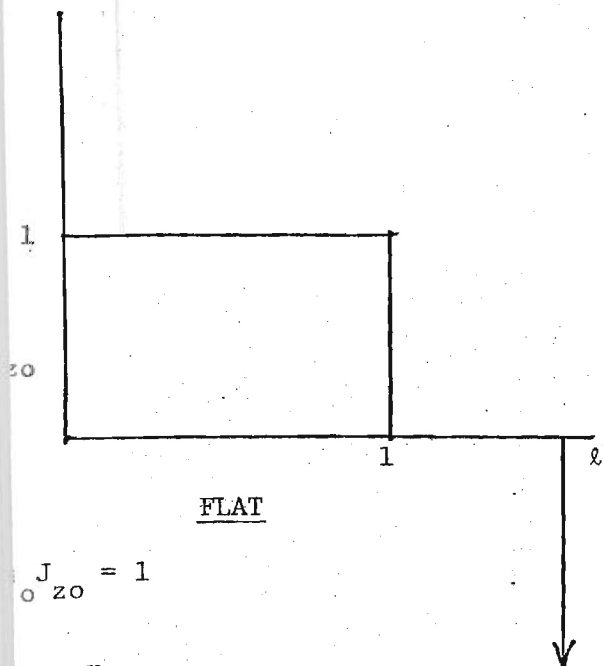
along magnetic field lines. Thus the resistivity profile across the island will be constant. Since the large aspect ratio limit is being considered, the longitudinal electric field would be, to leading order, constant across the width of the island. Thus the current density would be constant along an island and, in the large aspect ratio limit, J_{z0} would be zero at the rational surface. This is ideal since it cancels out the singularity.

The remaining problem is the boundary value nature of the equation. Since J_{z0} is constant along the island width and the island width is one parameter to be determined, the island width will effectively function as a nonlinear eigenvalue. The width of the island is varied until a solution is found; since B_r and the width are related, the amplitude of B_r is also determined, thus completing the solution [12,13,14].

A detour to energy considerations will offer evidence for the "flattening" modification of the background equilibrium. Consider two radically different profiles - one very flat and the other so very highly peaked that it can be approximated as shown in Figure 4-1. Since the tokamak is a constant current device both current densities have been normalized. A coaxial conductor at 1 carries a current in the opposite direction so that the magnetic field at 1+ is zero. (This avoids the problem of infinite fields in the cylinder case.) It is apparent from Equations (a) and (b) in Figure 4-1 that the more peaked current profile has the greater inductance thus more energy. One can speculate that the magnetic islands could act as a mechanism to spread out the current profile and thus lower the magnetic energy stored in the plasma.

The question of the validity of this axisymmetric "flattening" arises. Clearly, if the islands overlap an annular "destroyed" region would exist and this apparently axisymmetric modification of the equilibrium would be appropriate; however does this also apply to the single island case? This problem is addressed by the fact that while the perturbed terms are small, the derivatives of the background equilibrium quantities, specifically the pressure, are also small and thus the perturbed terms can greatly modify the topology of the area in close proximity of the island center. This may be thought of as an analogue to the boundary layer behavior in Chapter 1.

(a)

FLAT

$$J_{zo} = 1$$

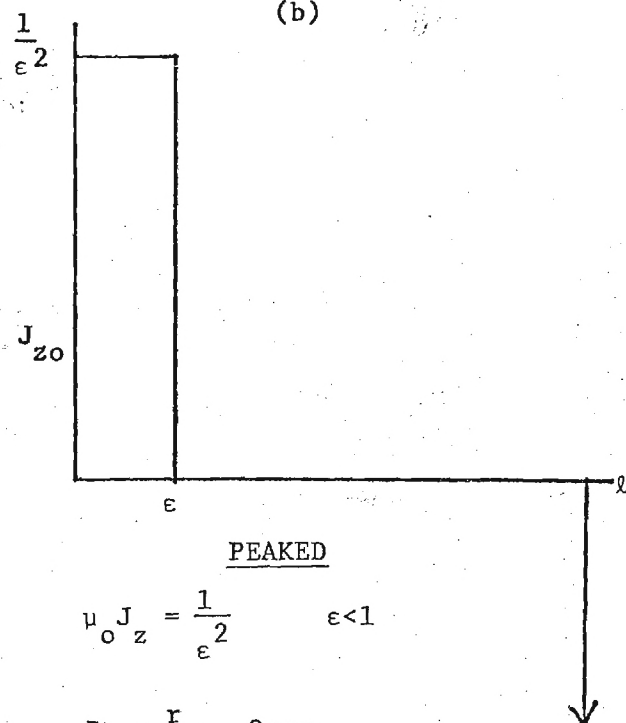
$$B_{\theta} = \frac{r}{2} \quad 0 < r < 1$$

$$B_{\theta} = \frac{1}{2r} \quad 1 < r < l$$

$$L_2 \sim \int_0^1 \frac{r^3}{4} dr + \int_1^l \frac{1}{4r} dr$$

$$\frac{L_2}{L_1} = \frac{\frac{1}{16} + \frac{1}{4} \ln \frac{l}{\epsilon}}{\frac{1}{16} + \frac{1}{4} \ln l} > 0$$

(b)

PEAKED

$$J_{zo} = \frac{1}{\epsilon^2} \quad \epsilon < 1$$

$$B_{\theta} = \frac{r}{2\epsilon^2} \quad 0 < r < \epsilon$$

$$B_{\theta} = \frac{1}{2r} \quad \epsilon < r < l$$

$$L_2 \sim \int_0^{\epsilon} \frac{r^3}{4\epsilon^4} dr + \int_{\epsilon}^l \frac{1}{4r} dr$$

[Coaxial Conductor at l carries A Current- I so that $B = 0$ at l^+]

Figure 4-1. Inductance of peaked and flat current profiles.

The solution to (38) is not unique; solutions are possible with several different island combinations. Like the solutions to the reduced MHD equations, this model is also very sensitive to the initial background current profile [2].

A quasilinear model has been developed to determine the saturated tearing mode amplitudes in axisymmetric toroidal geometry with no assumptions on the cross-sectional shape, aspect ratio, or beta [14]. This model relies on a transformation of the MHD equilibrium to Hamada coordinates and the exploitation of a relationship between contravariant and covariant vector components [49]. This selection produces a relatively simple pair of ordinary differential equations for each helical component. Fourier harmonic mixing only occurs when evaluating the driving terms for these differential equations, thus producing a tractable computational set.

Another approach to the tearing mode problem is to use an energy method to determine the stability threshold of the tearing modes [3,8,15,43,48]. This method leads to the minimization of an energy integral and an Euler equation which can be solved in a way similar to the previously mentioned Δ' analysis. This Euler equation can also be numerically expressed in a finite element form which leads to a matrix eigenvalue problem. The singular nature of the problem does show up however, leading the authors to evaluate the resulting integrals in a principle value sense with the assumption of a non-vanishing gradient of the safety factor at the singular surface. This type of integral evaluation is related to the Δ' type of formulation; the apparent difference arises from the different norms used in the minimization [3,48]. The principle value evaluation of the integrals removes the discontinuity by effectively subtracting out the Δ' singularity. The energy methods have been used to examine the effect of plasma shape on poloidal coupling of tearing modes. The background current profile was assumed to be bell-shaped and the plasma was D shaped. It was found that initially the 2/1 and 3/2 modes are unstable; if one tries to flatten the current profile to stabilize them, higher m modes can be excited. This behavior is similar to the reduced MHD cases in which stable and unstable harmonics interact to destabilize stable harmonics. It was also found that a stable current configuration can be obtained by reducing the current gradient between the $q = 1.5$ and $q = 2.0$ surfaces and making it sharper for $q > 2.0$. This is also consistent with other models; the functional form near the island is very important [48]. While this model has included the effects of plasma shaping, it is still a large aspect ratio approximation.

The quasilinear and energy models effectively trade the time dependent nature of the problem for gains in the geometric complexity.

5. SUMMARY

Magnetic islands, being resonance phenomena, can have large scale effects on the plasma even though the amplitudes of the modes themselves are small. They are believed to cause the major disruption by connecting the center of the plasma to the limiter or by the overlap of two different islands which destroys the magnetic confinement. In either case, the transport losses become so high that the discharge can no longer be sustained. Their existence can also explain the sawtooth like oscillations in the center of the plasma which flattens the pressure and temperature profiles there. Mirnov oscillations, which are relatively benign and usually do not cause termination of the discharge, are also an effect of the tearing mode instability and are caused by the rotation of the magnetic islands.

An equilibrium with magnetic islands may be a lower energy configuration, thus making it a favorable state for a dissipative system. Analogous systems in classical mechanics have been shown to have a distorted and destroyed phase space torus; the KAM theorem provides insight to this behavior and some of the theoretical justification of the magnetic island model of MHD equilibrium.

Magnetic islands were first examined in a plane slab geometry. This analysis showed that boundary layer like behavior occurred in the region at the island center and that special care was needed in producing a solution. The reduced MHD equations were developed in order to include the geometric effects of more physical cases. These equations showed that the effect of toroidal and poloidal coupling was significant and complex. Furthermore, these tearing modes were found to be very sensitive to the current profile, thus adding a further parameter to the situation. An energy formulation of the tearing mode model was also examined and it provided results that were consistent with the other models with the advantage of being able to handle a larger number of modes. It was, however limited only to the time independent case and was linear rather than a quasilinear or nonlinear formulation.

A quasilinear model was developed in order to examine the saturated island case and the influence of the island on the background equilibrium. Early models examined the large aspect ratio case and future models will be able to examine the finite aspect ratio case, thus allowing more physical problems to be examined.

References

1. L. S. Solov'ev, V. D. Shafranov, Reviews of Plasma Physics, Volume 5, Consultants Bureau, New York, 1, (1970).
2. G. Bateman, MHD Instabilities, The M.I.T. Press, Cambridge, 1978.
3. J. D. Callen, et al., "Magnetic Islandography in Tokamaks," Oak Ridge National Laboratory, ORNL/TM-6564.
3. H. P. Furth, P. H. Rutherford, H. Seiberg, Phys. Fluids, 16, 1054, (1973).
4. B. B. Kadomtsev, O. P. Pogutse, Sov. Phys-JETP, Vol. 38, 283, (1974).
5. J. L. Johnston, J. M. Greene, Plasma Physics, 9, 611, (1967).
6. A. H. Glasser, J. M. Greene, J. L. Johnson, Phys. Fluids, 18, 875, (1975).
7. A. H. Glasser, J. M. Greene, J. L. Johnson, Phys. Fluids, 19, 567, (1976).
8. H. Tasso, J. T. Virtamo, Plasma Physics, 22, 1003, (1980).
9. R. B. Paris, "Lectures on Resistive Instabilities in MHD", Department de Recherches Sur La Fusion Controlee, Association Euratom - C.E.A. (February 1982).
10. P. H. Rutherford, H. P. Furth, "Nonlinear Properties of Kink and Tearing Instabilities in Tokamaks", MATT-872, Plasma Physics Laboratory, Princeton University (December 1971).
11. R. B. White, "Resistive Instabilities and Field Line Reconnection", Princeton University, PPPI-1655
12. G. Bateman, R. N. Morris, "Effect of a Localized Magnetic Perturbation on Magnetic Islands in a Cylindrical Plasma", Georgia Institute of Technology Fusion Report GTFR-15 (May 1980).
13. R. B. White, D. A. Monticelo, M. N. Rosenbluth, B. V. Waddell, Phys. Fluids, 20, 800, (1977).
14. G. Bateman, R. N. Morris, "Model for Saturated Tearing Modes in Toroidal Geometry", Georgia Institute of Technology Fusion Report GTFR-31, (April 1982).
15. W. Kerner, H. Tasso, Plasma Physics, 24, 97 (1982).
16. K. Toi, K. Sakurai, S. Tanahashi, S. Yasue, "Soft and Hard Major Disruption in the Profile Control Experiment of the JIPP T-II Tokamak", Institute of Plasma Physics, Magoya University Research Report IPPJ-547, (September 1981).
17. H. R. Hicks, J. A. Holmes, B. A. Carreras, D. J. Tetreault, G. Berge, J. P. Freidberg, P. A. Politzer, D. Sherwell, in Eight Int. Conf. on Plasma Physics and Controlled Nuclear Fusion Research (IAEA Brussels), Vol. I, 259 (1980).

18. H. R. Hicks, B. Carreras, J. A. Holmes, B. V. Waddell, "Interaction of Tearing Modes of Different Pitch in Cylindrical Geometry", Oak Ridge National Laboratory Report ORNL/TM-6096, (December 1977).
19. F. Karger, et al., in Sixth Int. Conf. on Plasma Physics and Controlled Nuclear Fusion Research (IAEA Berchtesgaden), Volume I, 267 (1976).
20. K. Bol, et al., in Seventh Int. Conf. on Plasma Physics and Controlled Nuclear Fusion Research (IAEA, Innsbruck) Volume I, 11 (1978).
21. N. R. Sauthoff, S. Von Goeler, W. Stodiek, Nucl. Fusion, 18, 1445 (1978).
22. B. V. Waddell, B. Carreras, H. R. Hicks, J. A. Holmes, D. K. Lee, Phys. Rev. Lett., 41, 1386 (1978).
23. J. D. Callen, et al., in Seventh Int. Conf. on Plasma Physics and Controlled Nuclear Fusion Research (IAEA, Innsbruck) Volume I, 415 (1978).
24. B. V. Waddell, B. Carreras, H. R. Hicks, J. A. Holmes, Phys. Fluids, 22, 896 (1979).
25. B. Carreras, B. V. Waddell, H. R. Hicks, Nucl. Fusion, 19, 1423 (1979).
26. B. Carreras, H. R. Hicks, J. A. Holmes, B. V. Waddell, Phys. Fluids, 23, 1811 (1980).
27. A. Sykes, J. A. Wesson, Rev. Lett., 44, 1215 (1980).
28. J. A. Holmes, et al., "Tearing Mode Calculations for Noncircular Tokamak Plasmas", Proc. IEEE Int. Conf. on Plasma Science, Madison, Wisconsin, (May 1980).
29. B. Carreras, B. V. Waddell, and H. R. Hicks, "Poloidal Magnetic Field Fluctuations in Tokamaks", ORNL/TM-6403, (July 1978).
30. B. V. Waddell, G. L. Jahns, J. D. Callen, H. R. Hicks, Nucl. Fusion, 18, 735 (1978).
31. G. L. Jahns, M. Soler, B. V. Waddell, J. D. Callen, H. R. Hicks, Nucl. Fusion, 18, 609 (1978).
32. S. J. Zweben, B. V. Waddell, D. W. Swain, H. H. Fleischman, "High Energy Runaway Orbits in the Presence of $m=2$ Magnetic Islands", ORNL/TM-6126, July 1973.
33. M. V. berry in "Topics in Nonlinear Dynamics", (JORNA, S., ed.), (AM. Inst. Phys. New York) 16-120 (1978).
34. A. N. Koimogorov, in Proceeding of the International Congress of Mathematicians North Holland, Amsterdam, Vol. I, 315 1957.
35. V. I. Arnol'd, Russ. Math. Sor., 18, 9 1963.
36. J. Moser, Machr. Akad. Wiss Gottingen II Math. Phys. k1, 1 1962.
37. A. H. Boozer, R. B. White, "Particle Diffusion in Tokamaks with Partially Destroyed Magnetic Surfaces", Princeton University, PPPL-1872, 1982.

38. H. Goldstein, Classical Mechanics, 2nd Edition, Addison-Wesley Publishing Company, Reading Massachusetts
39. H. P. Furth, J. Killeen, M. N. Rosenbluth, Phys. Fluids, 6, 459 1963.
40. G. Schmidt, Physics of High Temperature Plasmas, 2nd Edition, Academic Press, New York, (1979).
41. H. R. Strauss, Phys. Fluids, 19, 134 1976.
42. H. Tasso, Plasma Physics, 17, 1131 1975.
43. R. B. White, D. A. Monticello, M. N. Rosenbluth, Phys. Rev. Letters, 39, (1977).
44. S. Yoskikawa, Phys. Rev. Letters, 27, (1971).
45. B. Carreras, H. R. Hicks, D. K. Lee, "The Effects of Toroidal Coupling on Stability of Tearing Modes," Oak Ridge National Laboratory Report ORNL/TM-7281, (1980).
46. D. Edery, J. L. Soule, R. Pellat, M. Frey, J. P. Somon, "Non-Linear Evolution of Tearing Modes in Toroidal Geometry", in Eighth Conference Proceedings on Plasma Physics and Controlled Nuclear Fusion Research, (IAEA, Brussels), Volume I, 269 (1980).
47. W. Kerner, H. Tasso, "Stability of Multihelical Tearing Modes in Shaped Tokamaks", Max-Planck-Institut Fur Plasmaphysik, IPP 6/211, (March 1982).
48. S. Hamada, Nuclear Fusion, 2, 22 1962.
49. P. H. Rutherford, Phys. Fluids, 16, 1903 (1973).
50. A. H. Mayfeh, Perturbation Methods, Wiley, New York, (1973).
51. M. N. Rosenbluth, D. A. Monticello, H. Strauss, R. B. White, Phys. fluids, 19, 1987, 1976.
52. D. Biskamp, H. Welter, "Numerical Studies of Resistive Instabilities", in Sixth Conference Proceeding on Plasma Physics and Controlled Nuclear Fusion Research (IAEA, Berchtesgaden), Vol. I, 579 1976.

APPENDIX A

It is instructive to see the type of magnetic field that causes magnetic islands and for the moment let us consider only the magnetic field - disregard the plasma current and force balance. For a specific example form the magnetic field from two components; first an axisymmetric part which is the major or dominate part (See Figure A-1 for the coordinate system).

$$B_{\phi} = \frac{B_o}{(R_o + r \cos \theta)} \quad (A1)$$

$$B_{\theta} = \frac{r(1 - Cr^2)}{(R_o + r \cos \theta)} \quad (A2)$$

where B_o , R_o , and C are constants.

The important characteristic of the field, with respect to the particles, is the field line configuration since the particles are forced to travel along it to a first approximation. A field line is defined as

$$\vec{B} \times d\vec{\ell} = 0 \quad (A3)$$

where $\vec{\ell}$ is a vector tangent to the field line. For this coordinate system

$$d\vec{\ell} = (R_o + r \cos \theta) d\phi \hat{\phi} + r d\theta \hat{\theta} + dr \hat{r} \quad (A4)$$

and becomes

$$r B_{\phi} d\theta - (R_o + r \cos \theta) B_{\theta} d\phi = 0 \quad (A5)$$

$$B_{\theta} dr - r B_{\phi} d\theta = 0 \quad (A6)$$

$$B_r (R_o + r \cos \theta) d\phi - B_{\phi} dr = 0 \quad (A7)$$

Since the axisymmetric part has no B_r component this set of equations simplifies to

$$\frac{d\theta}{d\phi} = \frac{(R_o + r \cos \theta)}{r} \frac{B_{\theta}}{B_{\phi}} \quad (A8)$$

By tracing out the field lines the shape of the flux surfaces that contain them can be determined. To do so map a magnetic surface by the following procedure:

1. Select a ϕ say ϕ_o
2. Follow the field line around until $\phi = \phi_o + 2\pi n$
3. Put an "x" on the plane at that point.

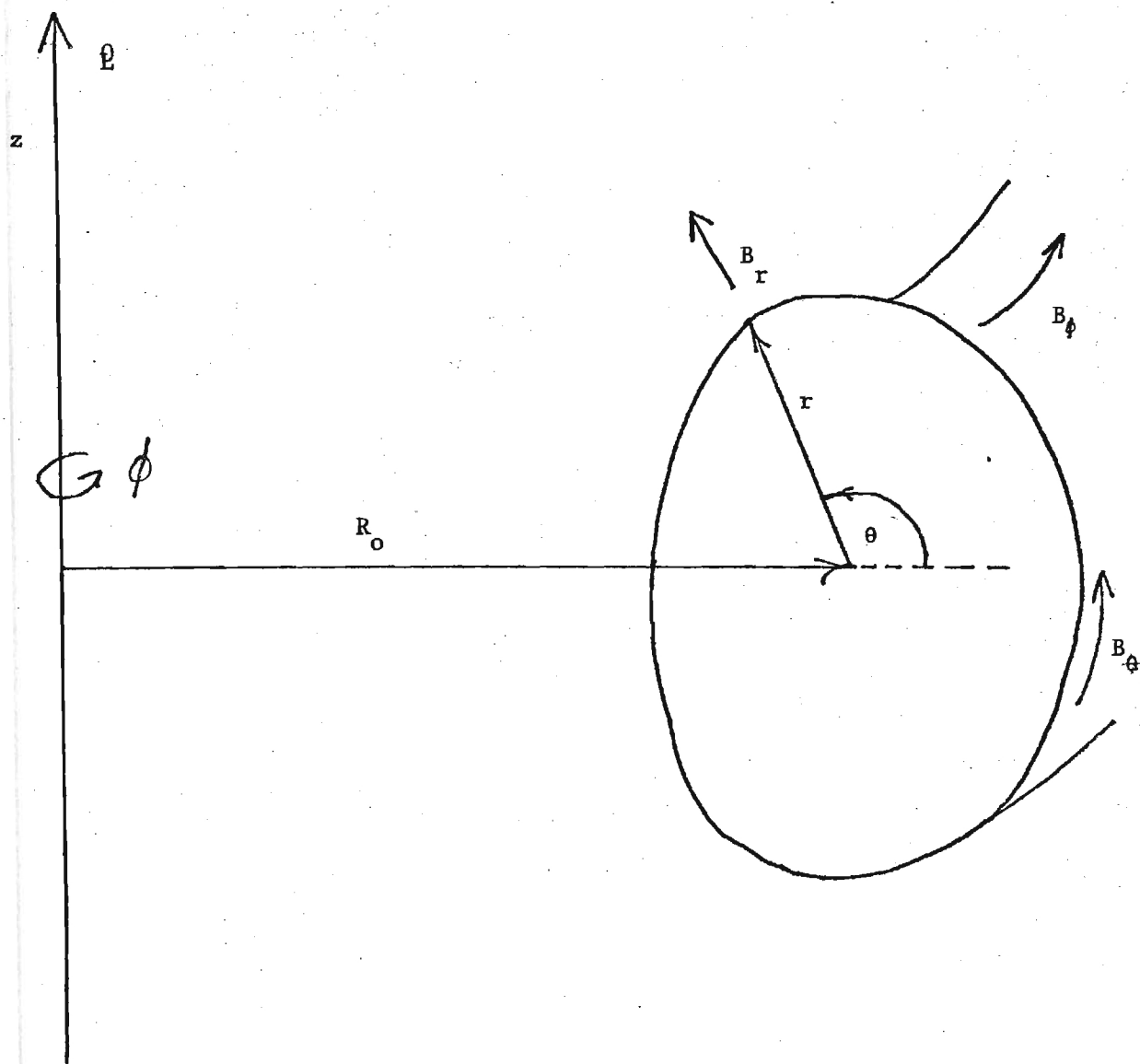


Figure A-1. Appendix A coordinate system.

4. Continue following the field line around and make "x"'s at ϕ where

$$\phi = \phi_0 + 2\pi n$$

This is known as a puncture plot and is shown in Figures A-2a and A-2b. As can be seen these maps are closed curves in all but a few cases. The field lines that close on themselves produce only a few dots, rather than closed curves. In order to outline a flux surface in this case, one needs to trace out an infinite number of field lines since one field line does not explore the entire surface. These field lines have the property that rotation in the ϕ direction divided by the rotation in the θ direction is an integer. The remaining surfaces do not have this property, thus the wandering about in θ which produces a magnetic surface. It is not surprising then to realize that the rotational transform (number of turns in the poloidal direction of a field line with the number of turns going to infinity) of a surface made up of closed field lines is also an integer. This is a crucial point.

Now consider a perturbation along the field line. With irrational field lines this perturbation would be spread out over a surface, but with rational field lines this perturbation ends up at the same place orbit after orbit. Thus rather than having its effect spread out or averaged over a surface, the effect is concentrated and enhanced by the rational nature of the surface. This is the source of the resonance behavior.

The Perturbation

Add to the axisymmetric background a perturbation of the form

$$B_r = \frac{A}{r(R_0 + r \cos \theta)} \cos(m\theta - n\phi)$$

where A is a constant and m and n are integers. From the illustration Figure A-3 one sees that not much is changed except near the regions where the pitch of the field line is the same as that of the perturbation or where

$$m\theta - n\phi = S$$

where S is a constant.

In those regions the phase of the perturbation is "locked" on to the field line and it pushes (or pulls) the field line in (or out) until it drifts far enough from the surface to lose phase altogether. It is this process that forms the island regions in the plasma. Both a radial magnetic field and a resonant magnetic field line are required to form an island [1,12].

Q AT R= .100 IS 1.753

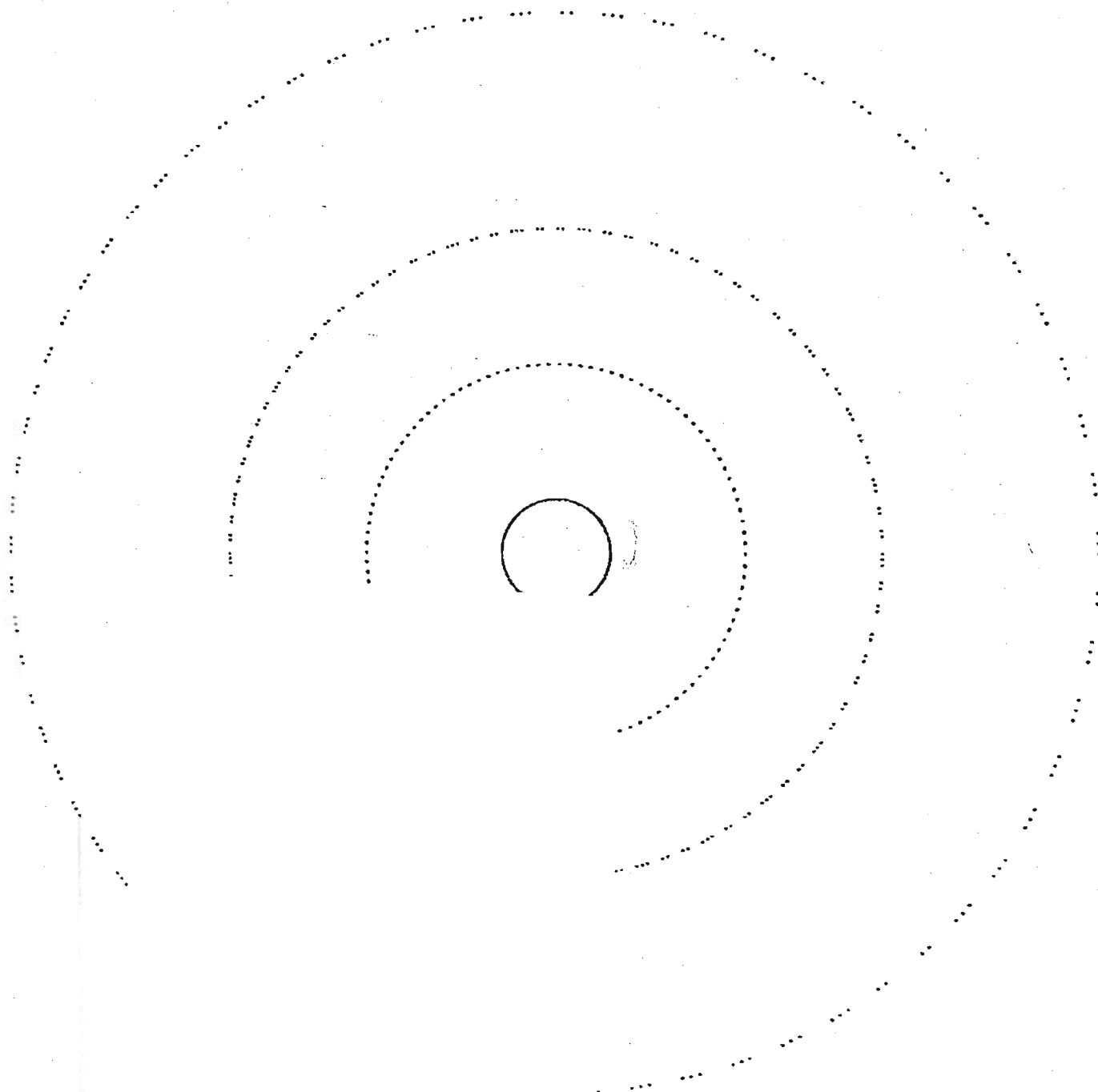
Q AT R= .350 IS 1.932

Q AT R= .600 IS 2.459

Q AT R=1.000 IS 8.875

RAD =5.000 B = 8.693 Z = .800

A2 = 0. A3 = 0.



ix surfaces.

Q AT R= .100 IS 1.753

Q AT R= .400 IS 2.000

Q AT R= .720 IS 3.003

Q AT R=1.000 IS 8.875

RAD =5.000 B = 8.693 Z = .800

A2 = 0. A3 = 0.

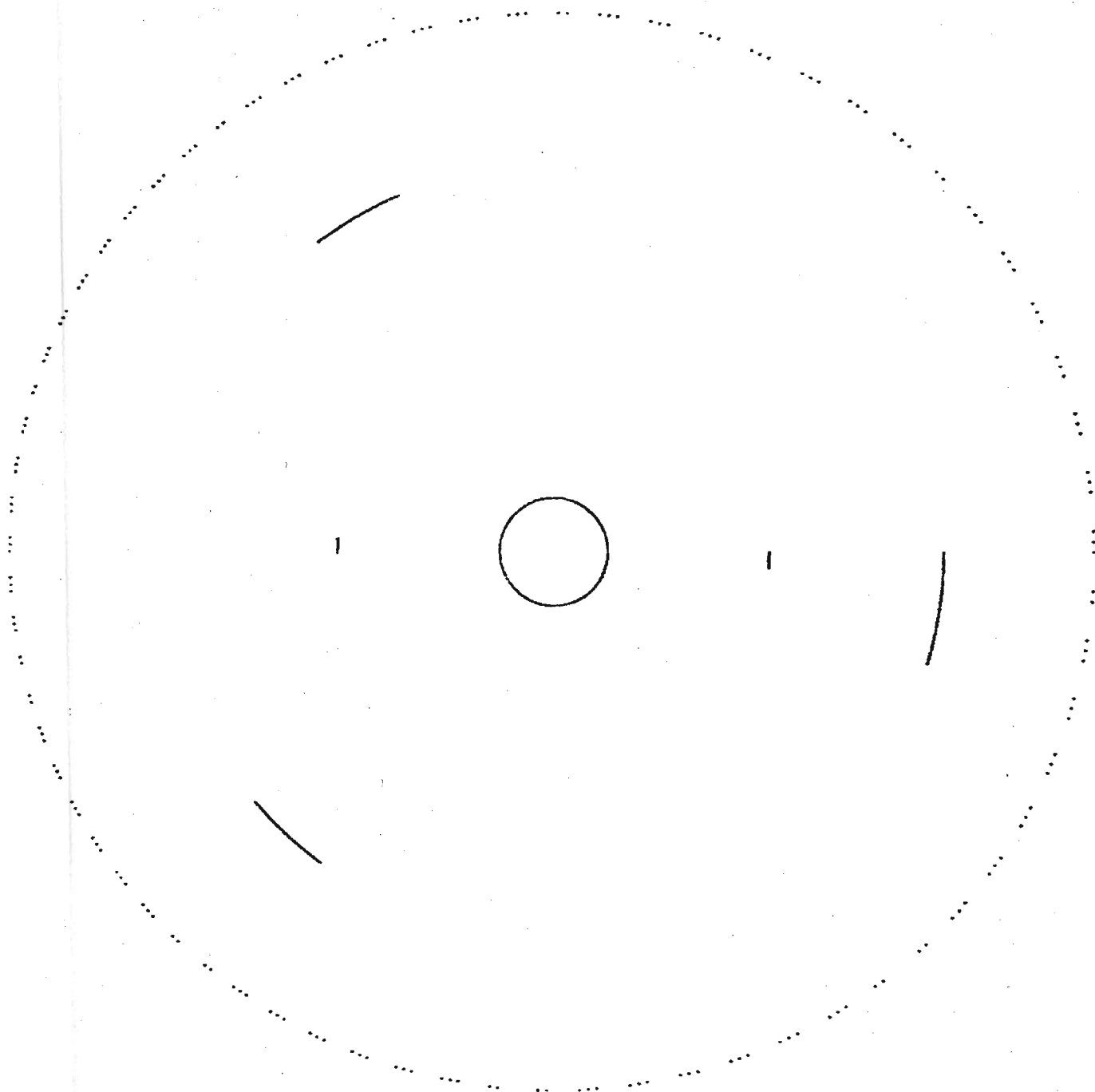


Figure A-2b. Rational vs Irrational
Flux Surfaces.

Q AT R= .100 IS 1.753

Q AT R= .400 IS 2.000

Q AT R= .720 IS 3.005

Q AT R=1.000 IS 8.875

RAD =5.000 B = 8.693 Z = .800

A2 = 3.00E-04 A3 = 0.

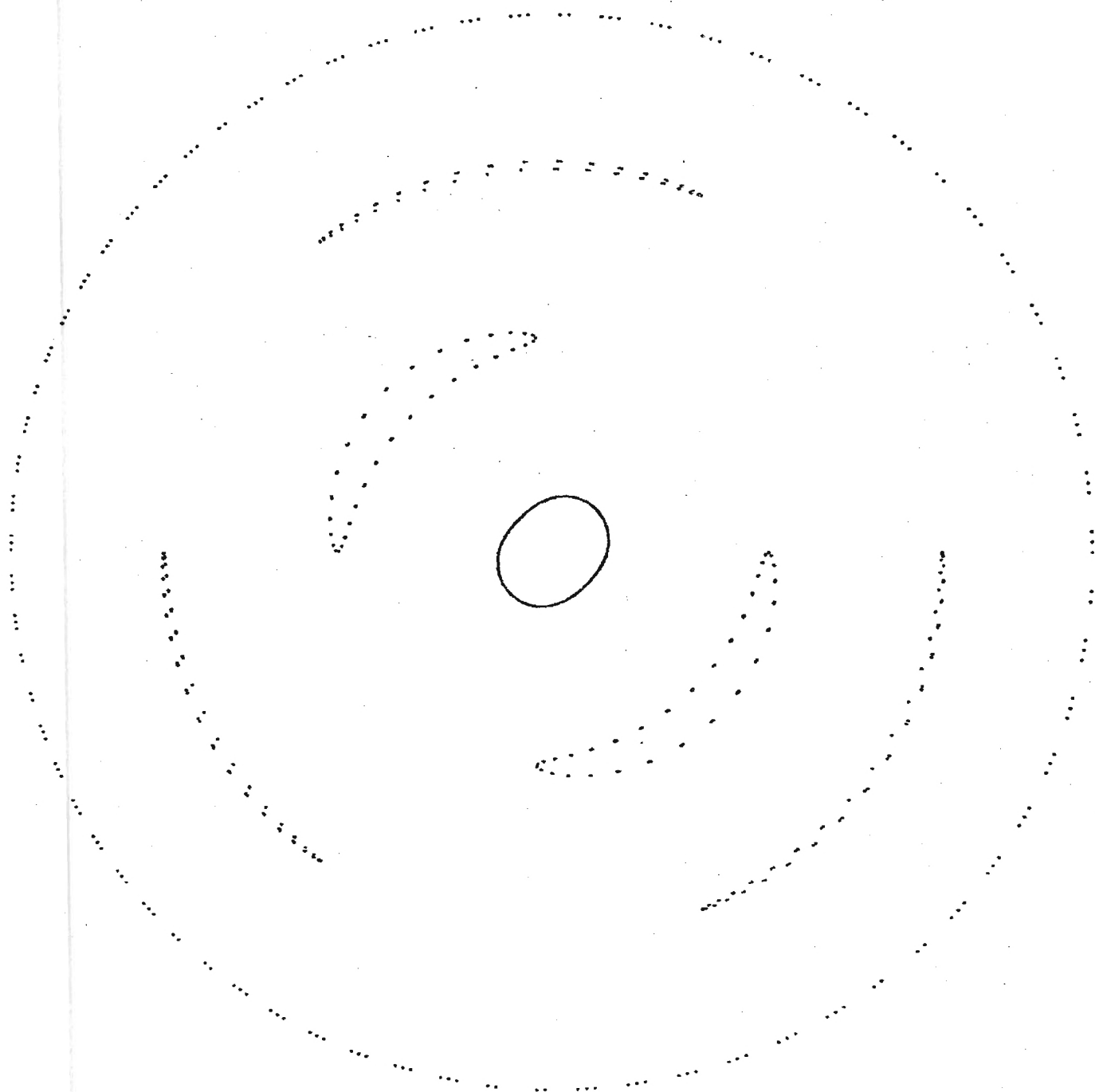


Figure A-3. Perturbed Flux Surfaces.

Since the boundary of the plasma is in approximately the same place that it was before the perturbation was added, the island forms a kind of transport short circuit that allows ions on the inner regions to travel to the outer regions, not via the slow diffusion process, but by the rapid velocity of particles along the field line.

Now consider another case: what if many islands of different helicity are present? Suppose both an $m=2, n=1$ ($2/1$) and $3/1$ island are present. If the perturbations are small enough, two chains of islands are formed as in Figure A-4. If however, the perturbations become strong enough so that the islands overlap, the situation takes on a chaotic nature [33] see Figure A-5. With some overlap, the field lines between the islands start to wander about as if they cannot decide whether they belong to the $3/1$ or the $2/1$ island. As the perturbation becomes even larger this wandering spreads out and eventually occupies a major part of the plasma. It is this type of pathology that is speculated to destroy the plasma confinement - the islands grow, then overlap and the plasma dumps. The exact mechanism is of course, more complicated, but the action is expected to be of this nature.

Q AT R= .400 IS 2.004

Q AT R= .600 IS 2.454

Q AT R= .720 IS 3.002

Q AT R=1.000 IS 8.872

RAD =5.000 B = 8.693 Z = .800

A2 = 1.50E-03 A3 = 2.50E-03

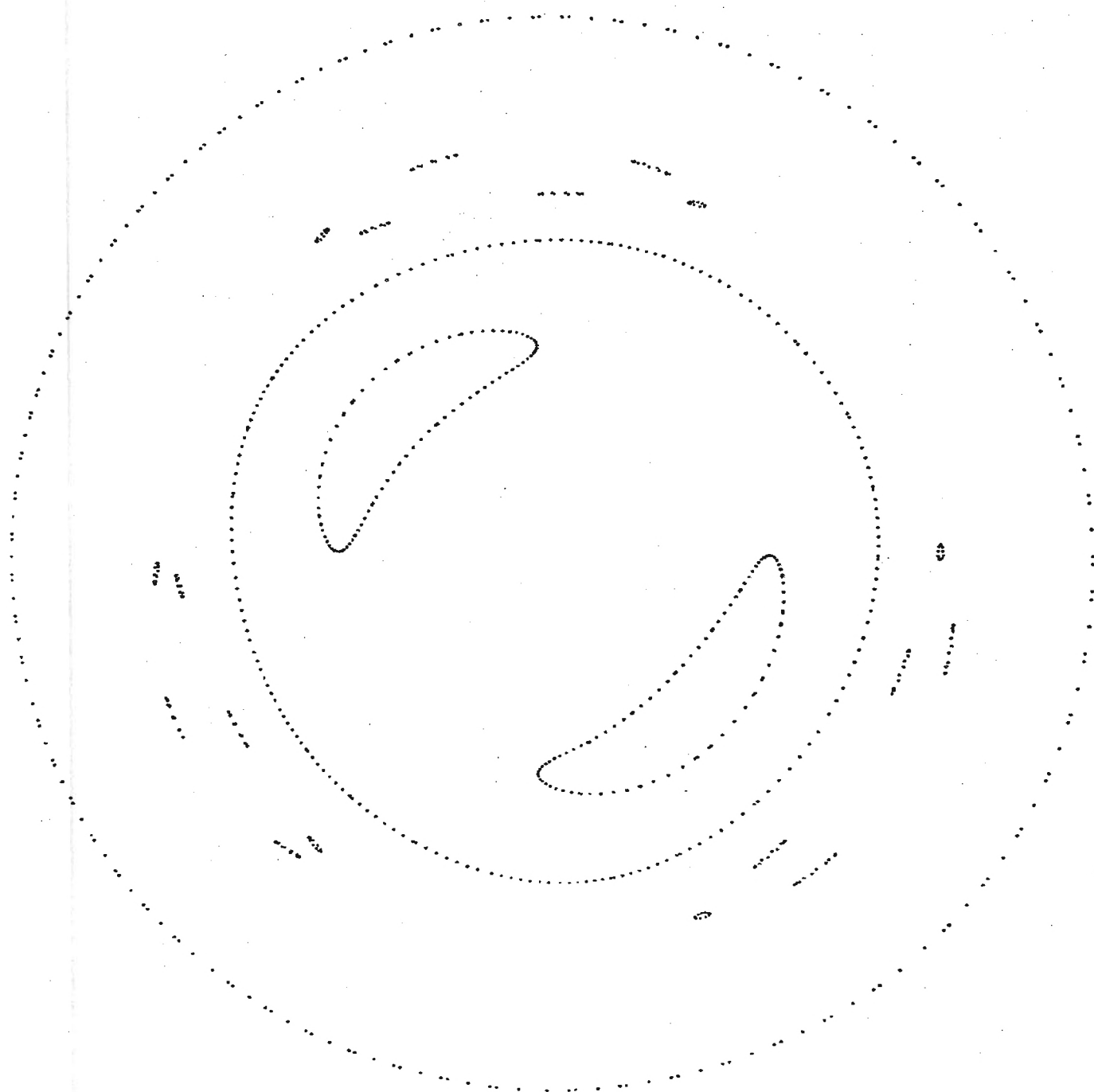


Figure A-4. Multiple Islands.

Q AT $R = .400$ IS 2.000

Q AT $R = .600$ IS 3.437

Q AT $R = .720$ IS 3.007

Q AT $R = 1.000$ IS 8.849

$RAD = 5.000$ $B = 8.693$ $Z = .800$

$A2 = 4.50E-03$ $A3 = 6.50E-03$



Figure A-5. Island Break Up.

APPENDIX B

The slab model of tearing modes is the simplest form possible for the study of tearing modes and the model is useful for gaining physical insight into the problems that are encountered [11,39,40].

To develop the set of equations to be used to solve for b_y (the magnetic field component responsible for the tearing mode) start with the force balance equation

$$\rho \frac{d\vec{v}}{dt} + \nabla p = \frac{(\nabla \times \vec{B}) \times \vec{B}}{\mu_0} \quad (B1)$$

and the magnetic diffusion equation

$$\frac{1}{\mu_0 \sigma} \nabla^2 \vec{B} + \nabla \times (\vec{v} \times \vec{B}) = \frac{\partial \vec{B}}{\partial t} \quad (B2)$$

Let the field be of the form

$$\vec{B} = B_x(y)\hat{x} + B_z(y)\hat{z} + \epsilon \left[b_x(y)\hat{x} + b_y(y)\hat{y} + b_z(y)\hat{z} \right] \exp \left[\gamma t + i(k_x x + k_z z) \right] \quad (B3)$$

$$\vec{v} = \epsilon \left[v_x(y)\hat{x} + v_y(y)\hat{y} + v_z(y)\hat{z} \right] \exp \left[\gamma t + i(k_x x + k_z z) \right] \quad (B4)$$

where $|\epsilon| \ll 1$

The variables are defined as:

- ρ plasma density
- \vec{v} perturbed fluid velocity
- p pressure
- \vec{B} background magnetic field
- \vec{b} perturbed magnetic field
- μ_0 permeability of free space
- σ conductivity
- γ linear growth rate

Proceed by taking the curl of (1) and then linearize the resulting equation

$$\rho \mu_0 \left[\nabla \times \frac{\partial \vec{v}}{\partial t} \right] = \nabla \times \left[(\vec{B} \cdot \nabla) \vec{b} + (\vec{b} \cdot \nabla) \vec{B} \right] \quad (B5)$$

Now linearize (2)

$$\frac{1}{\mu_0 \sigma} \nabla^2 \vec{b} + \nabla \times (\vec{v} \times \vec{B}) = \frac{\partial \vec{b}}{\partial t} \quad (B6)$$

By using components of these equations, one can produce an equation for b_y which is the objective of this section.

The important component of (6) is the y component

$$\frac{1}{\mu_0 \sigma} (b_y'' - k^2 b_y) + i v_y F = \gamma b_y \quad (B7)$$

where $k^2 = k_x^2 + k_z^2$ and $F = k_x B_x' + k_z B_z'$

From (5) the component of interest is the x component

$$i b_z' F + i b_z F' + b_y' B_z' + b_y B_z'' + k_z b_y F = \gamma \mu_0 \rho (v_z' - i k_z v_y') \quad (B8)$$

Also required is the z component of (5)

$$-k_x b_y F - i b_x' F - i b_x F' - b_y' B_x' - b_y B_x'' = \gamma \mu_0 \rho (i k_x v_y - v_x') \quad (B9)$$

Differentiate (8) by z and (9) by x and add to produce

$$i b_y F k^2 + i b_y F'' + i b_y' F' - F' (b_z k_z + b_x k_x) - F (k_x b_x' + k_z b_z') = \rho \gamma \mu_0 (i k_z v_z' + k_z^2 v_y + k_x^2 v_y + i k_x v_x') \quad (B10)$$

Assuming that $\nabla \cdot \vec{v} = 0$, (10) can be reduced to an equation involving only b_y and v_y . Add $-i(f \nabla \cdot \vec{b})'$ to the left hand side and $-\rho \gamma \mu_0 (\nabla \cdot \vec{v})'$ to the right hand side to produce:

$$i \rho \mu_0 \gamma (v_y'' - k^2 v_y) = -F b_y'' + k^2 F b_y + F'' b_y \quad (B11)$$

At long last, use (7) in (11)

$$\begin{aligned} & \delta^2 b_y^{(4)} - 2 \delta^2 \frac{F'}{F} b_y^{(3)} - \left[1 + 2k^2 \delta^2 + \delta^2 \frac{F''}{F} \right. \\ & \left. - 2 \delta^2 \left(\frac{F'}{F} \right)^2 + \frac{F^2}{\mu_o \rho_Y} \right] b_y'' + \frac{2F'}{F} (1 + k^2 \delta^2) b_y' \\ & - \left[2 \left(\frac{F'}{F} \right)^2 (1 + k^2 \delta^2) - \left(\frac{F''}{F} + k^2 \right) \left(1 + k^2 \delta^2 + \frac{F^2}{\mu_o \rho_Y} \right) \right] b_y \\ & = 0 \end{aligned} \quad (B12)$$

where $\delta^2 = \frac{1}{\mu_o \gamma \sigma}$

The cases of interest are the long wavelength modes or where $(k\delta)^2 \ll 1$.

Choosing some characteristic value L for the scale length one can see that $\delta^2 \frac{F''}{F} \sim \frac{\delta^2}{L^2}$ which is small compared to the other terms. Thus (12) can be reduced

$$\begin{aligned} \text{to: } & \delta^2 b_y^{(4)} - 2 \delta^2 \frac{F'}{F} b_y^{(3)} - \left[1 - 2 \delta^2 \left(\frac{F'}{F} \right)^2 + \frac{F^2}{\mu_o \rho_Y} \right] b_y'' \\ & + \frac{2F'}{F} b_y' + \left[\left(k^2 + \frac{F''}{F} \right) \left(1 + \frac{F^2}{\mu_o \rho_Y} \right) - 2 \left(\frac{F'}{F} \right)^2 \right] b_y \\ & = 0 \end{aligned} \quad (B13)$$

Far from the rational surface one would expect the δ^2 terms to be negligible since they involve resistive terms which are only important in the tearing layer (see below). The equation is then dominated by $\frac{1}{\mu_o \rho_Y^2}$ terms. Thus in the outer regions (13) becomes

$$b_y'' - \left(k^2 + \frac{F''}{F} \right) b_y = 0 \quad (B14)$$

Note that this equation is singular at the rational surface where $F = 0$. Also it is a boundary value problem with no eigenvalues to adjust. Unless F and F'' have some type of special behavior this equation cannot be used in the boundary layer region. (The boundary layer region is the region where equation (14) is singular.)

To examine the solution type near the rational surface, approximate F by the first term in a Taylor series expansion;

$$F \sim F_o' y \quad \frac{F'}{F} \sim \frac{1}{y} \quad F_o' \equiv F'(0) \quad (B15)$$

(13) is approximated near $F = 0$ by

$$\delta^2 b_y^{''''} - 2 \delta^2 \frac{b_y'''}{y} - \left[1 - \frac{2\delta^2}{y^2} + \frac{y^2 F_o'^2}{\mu_o \rho \gamma^2} \right] b_y'' + \frac{2}{y} b_y' + \left[k^2 \left(1 + \frac{y^2 F_o'^2}{\mu_o \rho \gamma^2} \right) - \frac{2}{y^2} \right] b_y = 0 \quad (B16)$$

Since the zero order equation cannot provide a sufficient solution to the problem, it is possible that the ordering has broken down in the region near the island center; that is, the derivative of the perturbation may not be small compared to the equilibrium quantities [51]. In that case rescale in the boundary layer with $w = y/\delta$ and keep only leading order terms

$$b_y^{''''} - \frac{2b_y'''}{w} - \left(1 - \frac{2}{w^2} + \beta^2 w^2 \right) b_y'' + \frac{2}{w} b_y' - \frac{2}{w^2} b_y = 0 \quad (B17)$$

$$\text{with } \beta^2 = \frac{\delta^2 F_o'^2}{\mu_o \rho \gamma^2}$$

(β is kept since $\mu_o \rho \gamma^2$ is also a small number).

Differentiate (17), multiply by $w/2$ and add back to (17) to produce the final form for the boundary region:

$$b_y^{''''} - (1 + \beta^2 w^2) b_y''' - 4 \beta^2 w b_y'' = 0 \quad (B18)$$

Near $w = 0$ this equation is not singular. For large w the asymptotic solutions are:

$$b_y'' \sim w^{-4} \quad (B19)$$

$$b_y'' \sim \exp \left[\pm \frac{1}{2} \beta w^2 \right] \quad (B20)$$

Since equation (14) is a second order equation one can expect b_y' to be continuous (but not necessarily b_y'') across the boundary region. The fact that the solution in the outer region changes on a scale length much greater than the inner solution indicates that b_y' of the outer solution is, on its scale length, constant across the boundary region. So $w \rightarrow \infty$ (that is, the boundary region meeting the outer solution) implies that b_y'' of the boundary layer solution must go to zero as $w \rightarrow \infty$ since b_y' of the outer solution is constant on that scale length [51]. Equations (19) and (20) both have this property so a solution over the entire plasma region is possible.

APPENDIX C

The reduced MHD equations form the backbone of many tearing mode studies and it is useful to outline the derivation of these equations and the approximations that were made [18,22].

Begin by assuming that the magnetic field can be written in the following way:

$$\vec{B} = \frac{-1}{R} \nabla \psi \hat{\zeta} + B_{\zeta} \hat{\zeta} \quad (C1)$$

where R is the radius (see Figure C-1).

$$R = R_0 + r \cos \theta \quad (C2)$$

in torodial geometry. Since $R \gg r$, the assumption that R is constant to leading order will be made. (This is a large aspect ratio approximation.)

The MHD equations are;

$$\rho \frac{d\vec{v}}{dt} = -\nabla p + \vec{J} \times \vec{B} \quad (C3)$$

$$\vec{J} = \nabla \times \vec{B} / \mu_0 \quad (C4)$$

$$\frac{\partial \vec{B}}{\partial t} = -\nabla \times \vec{E} \quad (C5)$$

$$\vec{E} + \vec{v} \times \vec{B} = \eta \vec{J} \quad (C6)$$

The variables are defined as;

ψ	flux function
\vec{A}	vector potential
ϕ	electrostatic potential
\vec{v}	fluid velocity
η	resistivity
\vec{E}	electric field
\vec{J}	current density
ρ	mass density
μ	permeativity of free space

To find the time dependence of ψ use equation (6) along with

$$\frac{\partial \vec{A}}{\partial t} = \nabla \phi - \vec{E} \quad (C7)$$

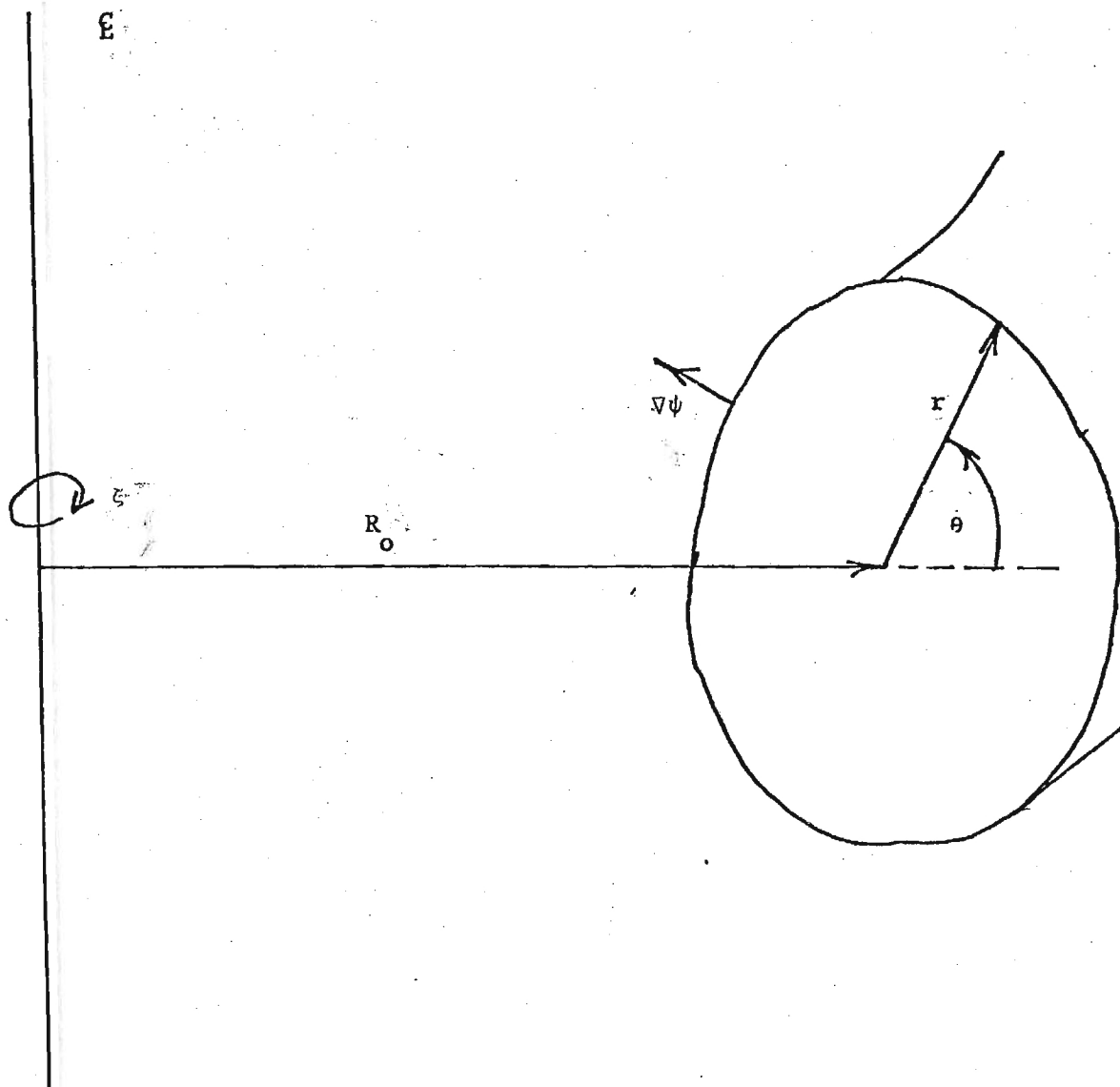


Figure C-1. Reduced MHD coordinate system.

from Maxwell's equations to produce

$$\frac{\partial \vec{A}}{\partial t} = \vec{v} \times \vec{B} - \eta \vec{J} + \nabla \phi \quad (C8)$$

Assuming that the vector potential has a form with $A_r \sim 0$ and A_θ small, the large aspect ratio approximation

for ψ is produced.

$$\psi = -RA_\theta \quad (C9)$$

Next dot $\hat{\zeta}$ into equation (8) using

$$\hat{\zeta} \cdot (\vec{v} \times \vec{B}) = \frac{\vec{v}_\perp \cdot \nabla \psi}{R} \quad (C10)$$

where \vec{v}_\perp is the velocity perpendicular to the magnetic field. The sum of these operations produces from equation (8)

$$\frac{\partial \psi}{\partial t} + \vec{v}_\perp \cdot \nabla \psi = \eta R J_\zeta - \frac{\partial \phi}{\partial \zeta} \quad (C11)$$

which is the desired equation for the time dependence of the flux.

The next desired quantity is J_ζ . Produce this by dotting $\hat{\zeta}$ into (4) and using the vector identity for $\nabla \cdot (\vec{G} \times \vec{F})$. This results in

$$\mu_0 J_\zeta = \nabla_\perp^2 \left(\frac{\psi}{R} \right) + \frac{\psi}{R^3} \quad (C12)$$

The last term is a toroidal effect and will be discarded in the cylinder limit.

To derive \vec{v}_\perp cross $\hat{\zeta}$ into equation (8) and discard the $\eta \vec{J}_\perp \times \hat{\zeta}$ term which is small. This produces

$$\vec{v}_\perp = \frac{1}{B_\zeta} (\nabla \psi \times \hat{\zeta}) \quad (C13)$$

The final equation is obtained by dotting $\hat{\zeta}$ into the curl of (3) after using the vector identity for $\nabla \cdot (\vec{F} \times \vec{G})$ and $\nabla \cdot (\vec{F} \cdot \vec{G})$. It is

$$\rho \left[\frac{\partial u}{\partial t} + \vec{v} \cdot \nabla u \right] = \frac{-(\nabla \psi \times \nabla J_\zeta) \cdot \hat{\zeta}}{R^2} - \frac{B_\zeta}{R^2} \frac{\partial J_\zeta}{\partial \zeta} + \frac{\vec{J}_\perp \cdot \nabla B_\zeta}{R} + \frac{\hat{z}}{R^2} \cdot (\vec{J} \times \vec{B}) \quad (C14)$$

with $u = (\nabla \times \frac{\vec{v}}{R}) \cdot \hat{\zeta}$ and small terms discarded. The last two terms in equation (14) are first order corrections in toroidal geometry. They are dropped in the cylinder limit.

These equations are used extensively in both the linear and nonlinear analysis. Before any further comments can be made, one needs to solve this set of equations in two particular limits.

Derivation of the Helical Flux Function

Define H as the helical flux function in cylindrical geometry and let [18,52]

$$H = \frac{-\psi}{R} - \frac{kr^2 B_{z0}}{2m}; \quad \bar{z} \Rightarrow z; \quad \mu_0 \Rightarrow 1 \quad (C15)$$

where k is a constant and m is an integer. This produces for ψ

$$\psi = -HR - \frac{kr^2 B_{z0}}{2m} \quad (C16)$$

The longitudinal current is then

$$J_z = -\nabla_{\perp}^2 H - \frac{2k}{m} B_{z0} \quad (C17)$$

The time evolution of the flux function becomes

$$\frac{\partial H}{\partial t} + \vec{v}_{\perp} \cdot \nabla H = \frac{dH}{dt} = 0 \quad (C18)$$

with

$$\nabla \cdot \vec{v}_{\perp} = 0 \quad (C19)$$

as before.

This set of equations form a two dimensional set which is useful for the study of a single tearing mode harmonic in a large aspect ratio limit.

Quasilinear Analysis Equations

In this case a magnetostatic limit is taken with [12]

$$\eta \Rightarrow 0, \quad \vec{v} \Rightarrow 0, \quad \phi \Rightarrow 0 \quad (C20)$$

It is derived in the cylindrical limit with

$$\hat{\zeta} \Rightarrow -R \hat{z}, \quad B_{\zeta} = B_{z0} \quad (C21)$$

This results in

$$-\mu_0 J_z = \nabla_{\perp}^2 \psi \quad (C22)$$

from (12) and

$$(\nabla \psi \times \nabla J_z) \cdot \hat{z} + B_{z0} \frac{\partial J_z}{\partial z} = 0 \quad (C23)$$

from (14).

To produce the radial magnetic field equation, which is the point of the derivation, let be written in the form

$$\psi = \psi_o(r) + \epsilon \psi_p(r, \theta, z) \quad (C24)$$

where $|\epsilon| \ll 1$. Using (22) and (23), keep zero order and first order terms:

$$-\mu_o J_{zo} = \nabla_{\perp}^2 \psi_o \quad (C25)$$

$$-\mu_o J_{zp} = \nabla_{\perp}^2 \psi_p \quad (C26)$$

$$\left[\left(\nabla \psi_o \times \nabla J_{zp} \right) + \left(\nabla \psi_p \times \nabla J_{zo} \right) \right] \cdot \hat{z} + B_{zo} \frac{\partial J_{zp}}{\partial z} = 0 \quad (C27)$$

Insert (26) into (27) using

$$\psi_p = f(r) \exp [i(m\theta - nkz)] \quad (C28)$$

To put this in the form used in reference [12] use

$$B_{\theta o} = \frac{\partial \psi_o}{\partial r} \quad (C29)$$

$$B_r = \frac{-imf}{r} \quad (C30)$$

$$\mu_o J_{zo} = \frac{1}{r} \frac{d}{dr} (r B_{\theta o}) \quad (C31)$$

This finally yields

$$\begin{aligned} \frac{d}{dr} \left(r \frac{d}{dr} r B_r \right) - m^2 B_r \\ + \frac{mr^2 \mu_o \frac{dJ_{zo}}{dr}}{(nrk B_{zo} - m B_{\theta o})} B_r = 0 \end{aligned} \quad (C32)$$

as the basic equation for the study of the radial field.

APPENDIX D

To examine the effect of magnetic islands upon the topology of the plasma confinement consider the equation for magnetic surfaces

$$\nabla \psi \cdot \vec{B} = 0 \quad (D1)$$

where \vec{B} is the magnetic field and ψ is a flux surface map. While this equation, in conjunction with the MHD equations, may have many solutions, the ones of principle interest form a set of simply nested flux surfaces [1].

If one departs from the simply nested flux surface model ψ may be forced to take on a very complicated form. The problem at hand is: given a magnetic island, find the simplest form that ψ can take on consistent with a physical interpretation.

To address this problem let

$$\vec{B} = \tau B^{0\theta} (\nabla \zeta \times \nabla v) + \tau B^{0\zeta} (\nabla v \times \nabla \theta) + \tau B^{1v} (\nabla \theta \times \nabla \zeta) \quad (D2)$$

where

- θ is the poloidal angle
- ζ is the toroidal angle
- v is the radial coordinate
- τ is the jacobian

$B^{0\theta}, B^{0\zeta}$ are the background equilibrium and B^{1v} is the perturbed radial field (first order correction) of the form

$$B^{1v} \sim \sum_{mn} B_{mn}^{1v} \exp [i(m\theta - n\zeta)]$$

Also let

$$\psi = \psi^0(v) + i\psi_{mn} \exp [i(m\theta - n\zeta)] \quad (D3)$$

where ψ_{mn} is the perturbed term. Use (2) and (3) in (1) to produce for a single harmonic (isolated island)

$$\frac{1}{(nB^{0\zeta} - mB^{0\theta})} \frac{d\psi^0}{dv} = \frac{-\psi_{mn}}{B_{mn}^{1v}} \quad (D4)$$

Since only the behavior of ψ^0 near $v = v_{mn}$ is of interest (rational surface) replace v with $v_{mn} + X$ where $X = v - v_{mn}$. Introduce $q = B^{0\theta}/B^{0\zeta}$ and rewrite (4) as

$$\frac{1}{(nq - m)} \frac{d\psi^0}{dv} = \frac{-\psi_{mn} B^{0\theta}}{B_{mn}^{1v}} \quad (D5)$$

Now, taking the limit of the right hand side of equation (5) and assuming that the left hand side is approximately constant across the island, the following second order equation is produced:

$$\frac{d^2 \psi^o}{dx^2} = \frac{-n \frac{dq}{dv}}{B_{mn}^{lv}} B^{o\theta} \psi_{mn} \quad (D6)$$

In this case one gets for ψ^o (with the condition that $\frac{d\psi^o}{dv}(o) = 0$),

$$\psi^o = \psi_o - \frac{n \frac{dq}{dv} B^{o\theta} \psi_{mn}}{2 B_{mn}^{lv}} x^2 \quad (D7)$$

where ψ_o is a constant. Thus near the island center ψ has a parabolic profile, which was to be expected since the magnetic island connects plasma on either side of the rational surface, forming an even function across the rational surface.

Using (7) in (3) and taking only the real parts one gets for ψ :

$$\psi = \psi_o - \frac{n \frac{dq}{dv} B^{o\theta}}{2 B_{mn}^{lv}} \psi_{mn} x^2 - \psi_{mn} \sin \alpha \quad (D8)$$

where $\alpha = (m\theta - n\zeta)$

See Figure D1. To determine the halfwidth of the island set the value of ψ at the seperatrix equal to that at the edge of the island

$$\psi(\alpha_s, x=0) = \psi(\alpha_H, H) \quad (D9)$$

of using (8)

$$H = \left[\frac{2 B_{mn}^{lv}}{n B_{mn}^{o\theta} \frac{dq}{dv}} (\sin \alpha_s - \sin \alpha_H) \right]^{1/2} \quad (D10)$$

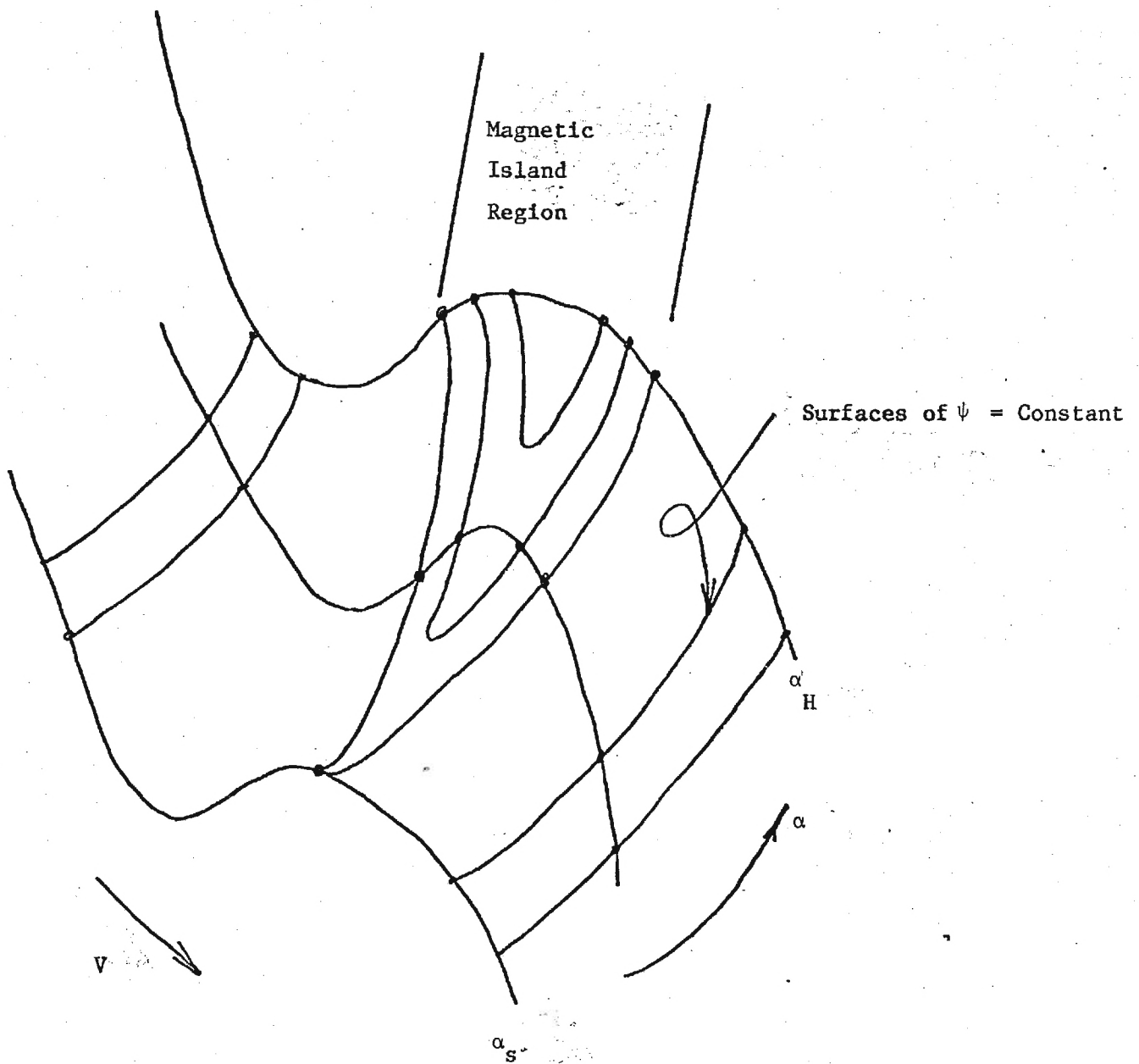


Figure D-1. Pressure in a magnetic island.

where

α_s is the value of α at the separatrix

α_H is the value of α at the half width

The maximum excursion occurs when

$$\alpha_s = \pi/2, \quad \alpha_H = 3\pi/2$$

giving for the half width

$$H = 2 \left(\frac{B_{mn}^{lv}}{nB^{o\theta} \frac{dq}{dv}} \right)^{1/2} \quad (D11)$$

with all quantities evaluated at $V = V_{mn}$

This result is in good agreement with computer experiments. [12].

GEORGIA TECH RESEARCH CORPORATION

GEORGIA INSTITUTE OF TECHNOLOGY
ATLANTA, GEORGIA 30332-0420

Telex: 542507 GTRCOCAATL
Fax: (404) 894-3120

Phone: (404) 894-4820

May 20, 1986

MEMORANDUM:

TO: Pat Heitmuller-CSD
FROM: Mildred Heyser
SUBJECT: E-26-675/E25-678

I am enclosing two copies of report on subject project that was submitted to me by Dr. W. M. Stacey as a final report.

I have this date submitted a copy to sponsor.

MH/wvs

Enclosures

saturated tearing modes in toroidal geometry

Glenn Bateman

Plasma Physics Laboratory, Princeton University, Princeton, New Jersey 08544

R. N. Morris

Oak Ridge National Laboratory, Oak Ridge, Tennessee 37830

(Received 11 April 1985; accepted 5 November 1985)

A quasilinear method is developed for determining saturated tearing mode magnetic island widths in axisymmetric toroidal plasmas with arbitrary cross-sectional shape, aspect ratio, or plasma pressure (β). The method is applied to compute magnetic island widths in force-free toroidal plasmas with aspect ratio as low as 2.0 and elongation between 1.0 and 2.0. It is found that current suppression within the magnetic island strongly increases the saturated width while current peaking reduces width. The effects of current profile, geometry, and harmonic mixing are also studied.

INTRODUCTION

Tearing modes have been studied almost exclusively in the large-aspect-ratio, low-beta limit using the reduced magnetohydrodynamic (MHD) equations.¹⁻³ These equations have been used in time-dependent computer codes to study the linear growth rate and nonlinear saturation rate.^{1,2,4-19} The island structures that are produced spontaneously by resistive tearing modes are believed to be responsible for disruptive instabilities, Mirnov oscillations, and for some part of the enhanced transport in tokamak experiments.

Major disruptions are of particular importance. They are believed to be caused by the overlap of magnetic islands with different helicity, which abruptly results in a stochastic magnetic region across which plasma confinement is lost.⁴⁻¹⁹ Under different conditions the $m/n = 1/1$, $2/1$, and $3/2$ islands overlap in various combinations to produce hard and soft disruptions.^{13,14,18} It has been found (using the reduced MHD equations) that toroidicity and elongation of the plasma cross section both have the effect of modifying the saturated tearing mode island widths as well as coupling various helical harmonic modes together.

The reduced MHD equations are a low-beta, large-aspect-ratio approximation that may not prove adequate for further analysis of tokamaks and spheromaks, since the next generation of machines, and most certainly commercial reactors, will be high-beta, low-aspect-ratio designs. This paper addresses that fact by developing a set of quasilinear ordinary differential equations for steady-state saturated tearing modes without making a low-beta or large-aspect-ratio approximation. The only expansion parameter used in this paper is the ratio of magnetic island width to plasma minor radius. The effect of magnetic islands on the background current profile and the mode-mixing effects of geometry are explicitly computed. The destruction of some magnetic surfaces because of secondary resonance can also be included in this quasilinear model. Fully nonlinear interactions of close magnetic islands are omitted.

The key to this derivation is the transformation of the MHD equilibrium to Hamada coordinates and the exploitation of a relationship between contravariant and covariant components. This selection of coordinates produces a rela-

tively simple pair of ordinary differential equations for each helical harmonic of the perturbation. Fourier convolution sums are needed only when evaluating the driving terms for these differential equations. The magnetic island widths act like nonlinear eigenvalues for the solution of these perturbed equations as two-point boundary-value problems. This method is developed in Secs. II and III, and computed examples are presented in Sec. IV.

II. THREE-DIMENSIONAL EQUILIBRIUM EQUATIONS

A tractable system of ordinary differential equations will be derived in this section for the solution of the three-dimensional, scalar-pressure plasma equilibrium force-balance equations

$$\mathbf{J} \times \mathbf{B} = \nabla p, \quad (1)$$

$$\mu_0 \mathbf{J} = \nabla \times \mathbf{B}, \quad (2)$$

$$\nabla \cdot \mathbf{B} = 0, \quad (3)$$

as a perturbation about an axisymmetric equilibrium. The equilibrium equations are linearized to first order in the perturbed magnetic field, which is effectively an expansion in the ratio of the square of the magnetic island width to the plasma radius. A nonlinear effect (more accurately a quasilinear effect) is considered in the next section, where it is shown that the magnetic islands flatten the background axisymmetric profiles at mode-rational surfaces. This effect removes an apparent singularity from the linearized equations at each mode rational surface. An iterative algorithm is then developed in which the widths and shapes of the magnetic island serve effectively as eigenvalues for the solution of the ordinary differential equations as two-point boundary-value problems.

The formalism developed here is specifically tailored to the study of magnetic islands formed by saturated tearing modes together with applied magnetic fields. Since magnetic islands are flux tubes that form around mode-rational magnetic surfaces, the derivation is carried out in flux coordinates defined in terms of the axisymmetric unperturbed equilibrium. For reasons that will be described below, this particular derivation produces a tractable set of equations only in Hamada coordinates²⁰⁻²² (V, θ, ζ) , in which V is a surface quantity, θ is an anglelike variable around the poloi-

dal direction (short way around), and ζ is an anglelike variable around the toroidal direction (long way around). The variable V may stand for the volume of the unperturbed magnetic surfaces or for any monotonically increasing or decreasing surface quantity.

The essential feature of Hamada coordinates is that the contravariant components of both the magnetic field and the current density are surface quantities

$$\mathbf{B}^0 \cdot \nabla \theta = B^{0\theta}(V), \quad \mathbf{B}^0 \cdot \nabla \zeta = B^{0\zeta}(V), \quad \mathbf{B}^0 \cdot \nabla V = 0, \quad (4)$$

$$\mathbf{J}^0 \cdot \nabla \theta = J^{0\theta}(V), \quad \mathbf{J}^0 \cdot \nabla \zeta = J^{0\zeta}(V), \quad \mathbf{J}^0 \cdot \nabla V = 0,$$

where \mathbf{B}^0 and \mathbf{J}^0 are the magnetic field and current density of the unperturbed (background) equilibrium, respectively. It follows from the equilibrium equations that the Jacobian (J) must then be a surface quantity

$$J \equiv (\nabla V \cdot \nabla \theta \times \nabla \zeta)^{-1} = J(V). \quad (5)$$

We further require that θ and ζ be periodic with period 2π for a straightforward generalization of the usual Hamada coordinates²⁰⁻²² in which the Jacobian and the periods are all unity. In our generalized Hamada coordinates, the force balance equation (1) reduces to

$$J(V) [J^{0\theta}(V) B^{0\zeta}(V) - J^{0\zeta}(V) B^{0\theta}(V)] = \frac{dp^0(V)}{dV}. \quad (6)$$

The derivation proceeds by writing the perturbed variables in both contravariant and covariant components:

$$\mathbf{B}^1 = B^{1V} \nabla \theta \times \nabla \zeta + B^{1\theta} \nabla \zeta \times \nabla V + B^{1\zeta} \nabla V \times \nabla \theta, \quad (7)$$

$$\mathbf{B}^1 = B^1_V \nabla V + B^1_\theta \nabla \theta + B^1_\zeta \nabla \zeta, \quad (8)$$

$$\mathbf{J}^1 = J^{1V} \nabla \theta \times \nabla \zeta + J^{1\theta} \nabla \zeta \times \nabla V + J^{1\zeta} \nabla V \times \nabla \theta. \quad (9)$$

All perturbed variables are then written as a series of Fourier harmonics of θ and ζ :

$$X^1(V, \theta, \zeta) = \sum_{m,n} X^1_{mn}(V) \exp(im\theta - in\zeta). \quad (10)$$

The divergence-free property of \mathbf{B}^1 [Eq. (3)] is most easily written in terms of the contravariant components of \mathbf{B}^1 [Eq. (7)]:

$$\frac{d}{dV} (-iJB^{1V}_{mn}) = nJB^{1\zeta}_{mn} - mJB^{1\theta}_{mn}. \quad (11)$$

Ampere's law for the perturbed current density [Eq. (2)], however, is most easily written in terms of the covariant components of \mathbf{B}^1 [Eq. (8)]:

$$\mu_0 J J^{1V}_{mn} = i(mB^1_{\zeta mn} + nB^1_{\theta mn}), \quad (12)$$

$$\mu_0 J J^{1\theta}_{mn} = -inB^1_{Vmn} - \frac{d}{dV} B^1_{\zeta mn}, \quad (13)$$

$$\mu_0 J J^{1\zeta}_{mn} = \frac{d}{dV} B^1_{\theta mn} - imB^1_{Vmn}. \quad (14)$$

The contravariant components of the current density and magnetic field are needed to write the perturbed force balance equation (1):

$$-J^{1V}_{mn} JB^{0\zeta} + J^{0\zeta} JB^{1V}_{mn} = imp^1_{mn}, \quad (15)$$

$$J^{1V}_{mn} JB^{0\theta} - J^{0\theta} JB^{1V}_{mn} = -inp^1_{mn}, \quad (16)$$

$$J^{1\theta}_{mn} JB^{0\zeta} - J^{1\zeta}_{mn} JB^{0\theta} + J^{0\theta} JB^{1\zeta}_{mn} - J^{0\zeta} JB^{1\theta}_{mn} = \frac{d}{dV} p^1_{mn}. \quad (17)$$

Either from these equations or from a linearization of $\mathbf{B} \cdot \nabla p = 0$, it can be shown that

$$(nB^{0\zeta} - mB^{0\theta}) p^1_{mn} = -iB^{1V}_{mn} \frac{dp^0}{dV}, \quad (18)$$

which can be used to eliminate p^1_{mn} in favor of B^{1V}_{mn} . The Fourier harmonic form of equilibrium equations [(15)–(18)] is greatly simplified by the choice of Hamada flux coordinates in which $B^{0\theta}, B^{0\zeta}, J^{0\theta}, J^{0\zeta}$, and J are all surface quantities.

At this point we are faced with a dilemma. Covariant and contravariant components are linearly related to each other by metric elements which are, in general functions of θ and V . The helical harmonics are therefore related by Fourier convolution series. If we try to write Eqs. (11)–(18) entirely in terms of contravariant (or covariant) components alone, the derivative will land on an involved linear combination of components and helical harmonics, resulting in an intractable system of differential equations.

If the mixed combination of contravariant and covariant helical harmonics ($-iJB^{1V}_{mn}, B^1_{\theta mn}$) is used as the set of primary variables, however, the dilemma is resolved and a relatively simple pair of ordinary differential equations can be derived for each helical harmonic. Fourier convolution sums are then needed only when evaluating the driving terms for these differential equations. Other variables, such as $B^1_{\zeta mn}$ and p^1_{mn} , can be eliminated algebraically. The decision to use $-iJB^{1V}_{mn}$ and $B^1_{\theta mn}$ as the primary variables is the crucial step needed to make this problem tractable.

Equation (12) is then used in Eq. (15) to obtain

$$mB^1_{\zeta mn} + nB^1_{\theta mn} = -iJB^{1V}_{mn} (\mu_0 J^{0\zeta} / B^{0\zeta}) - m(\mu_0 p^1_{mn} / B^{0\zeta}), \quad (19)$$

which can be used to eliminate $B^1_{\zeta mn}$ algebraically. Finally, Eq. (17) can be used together with Eqs. (13), (14), and (19) to derive

$$\begin{aligned} (nB^{0\zeta} - mB^{0\theta}) \left(\frac{d}{dV} B^1_{\theta mn} - imB^1_{Vmn} \right) \\ = \mu_0 (nJ^{0\zeta} - mJ^{0\theta}) JB^{1\zeta}_{mn} \\ - iJB^{1V}_{mn} B^{0\zeta} \frac{d}{dV} \frac{\mu_0 J^{0\zeta}}{B^{0\zeta}} \\ + m\mu_0 p^1_{mn} \frac{1}{B^{0\zeta}} \frac{d}{dV} B^{0\zeta}. \end{aligned} \quad (20)$$

Equations (11) and (20) form a coupled pair of ordinary differential equations for each helical harmonic of the variables $[-iJ(V)B^{1V}_{mn}(V), B^1_{\theta mn}(V)]$. Equations (18) and (19) are used to eliminate p^1_{mn} and $B^1_{\zeta mn}$. Algebraic relations for the variables $B^1_V, B^{1\theta}$, and $B^{1\zeta}$ are derived from Eqs. (7) and (8):

$$B^1_V = \frac{B^{1V}}{|\nabla V|^2} - B^1_\theta \frac{\nabla \theta \cdot \nabla V}{|\nabla V|^2} - B^1_\zeta \frac{\nabla \zeta \cdot \nabla V}{|\nabla V|^2}, \quad (21)$$

$$B^{1\theta} = B^{1\nu} \frac{\nabla\theta \cdot \nabla V}{|\nabla V|^2} + B_\theta^1 \left(|\nabla\theta|^2 - \frac{(\nabla\theta \cdot \nabla V)^2}{|\nabla V|^2} \right) + B_\xi^1 \left(\nabla\theta \cdot \nabla\xi - \frac{(\nabla\theta \cdot \nabla V)(\nabla\xi \cdot \nabla V)}{|\nabla V|^2} \right), \quad (22)$$

$$B^{1\xi} = B^{1\nu} \frac{\nabla\xi \cdot \nabla V}{|\nabla V|^2} + B_\theta^1 \left(\nabla\theta \cdot \nabla\xi - \frac{(\nabla\theta \cdot \nabla V)(\nabla\xi \cdot \nabla V)}{|\nabla V|^2} \right) + B_\xi^1 \left(|\nabla\xi|^2 - \frac{(\nabla\xi \cdot \nabla V)^2}{|\nabla V|^2} \right). \quad (23)$$

Fourier analysis of these equations results in convolution sums.

III. EFFECT OF MAGNETIC ISLANDS

At the mode rational surface $V = V_{mn}$ for any given helical harmonic, $q(V_{mn}) = m/n$, the expression

$$nB^{0\xi}(V) - mB^{0\theta}(V) = [nq(V) - m]B^{0\theta}(V) \quad (24)$$

passes through zero. Thus, Eqs. (18) and (20) appear to be singular at mode-rational surfaces. It will be shown in this section that $B_{mn}^{1\nu} \neq 0$ at a mode-rational surface implies the presence of a magnetic island or more complicated breakup of the mode-rational surface which, in turn, implies a flattening of the profiles $p^0(V)$ and $J^{0\xi}(V)/B^{0\xi}(V)$, which removes the singularity.²³⁻²⁸ This quasilinear treatment, in which the perturbation affects the background profile, permits the solution of the saturated, as opposed to just the linear, tearing mode problem. Only simple magnetic islands, each resulting from a single resonant helical harmonic, will be considered in this paper. Note that not all helical harmonics have mode-rational surfaces within the plasma. Given a driving term (an applied magnetic perturbation), the solution of Eqs. (11) and (20) for nonresonant helical harmonics is straightforward.

Consider any function ψ that is uniform along magnetic field lines:

$$\mathbf{B} \cdot \nabla\psi = 0. \quad (25)$$

Equation (25) implies nothing about the variation of ψ from one magnetic surface to the next, but let us take ψ to be a smooth function with a local minimum at the mode-rational surface being considered. The Taylor series for ψ satisfying Eq. (25) in the neighborhood of that mode-rational surface can be shown to be

$$\psi = \psi^0(V_{mn}) + \left(\frac{\psi_{mn}^1 n B^{0\theta}}{-2iB_{mn}^{1\nu} dV} \right) \bigg|_{V=V_{mn}} (V - V_{mn})^2 + \dots + \psi_{mn}^1 \exp(im\theta - in\xi). \quad (26)$$

From the real part of this expression, it can be shown that the half-width of the island is characterized by

$$H_{mn} \equiv V_S - V_{mn} = \pm 2 \left(\left| \frac{-iB_{mn}^{1\nu}}{nB^{0\theta}(dq/dV)} \right|_{V=V_{mn}} \right)^{1/2}, \quad (27)$$

where V_S refers to the unperturbed magnetic surface passing through the separatrix of the magnetic island at its widest

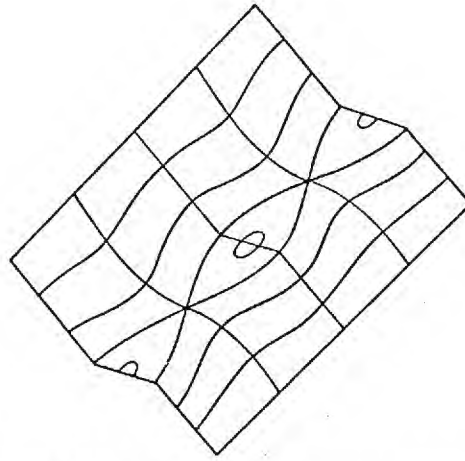


FIG. 1. Schematic illustration of pressure profile flattening due to the presence of a simple magnetic island.

point. The real part of ψ can then be written

$$\psi = \psi_{mn}^0 - 2\psi_{mn}^1 u^2 + \dots + \psi_{mn}^1 \cos(m\theta - n\xi), \quad (28)$$

where

$$u \equiv (V - V_{mn})/H_{mn}. \quad (29)$$

Higher-order terms in the Taylor series (26) may be used to determine the asymmetry in the island width and other details of the island's shape. Note that the island width is measured here in terms of the flux surface label V . The geometrical width of the island may vary poloidally around a flux surface, being wider where the background flux surfaces are more spread apart and narrower where the background flux surfaces are squeezed together. This effect is automatically taken into account when using flux coordinates.

Consider the pressure profile in the neighborhood of a magnetic island, which is determined by $\mathbf{B} \cdot \nabla p = 0$ to be uniform along magnetic surfaces and by transport considerations orthogonal to magnetic surfaces. Along a cut through the magnetic island at its widest point ($m\theta - n\xi = 0$), suppose that

$$p = \begin{cases} p_0 + p'_0 H_{mn}(u - 1), & u > 1, \\ p_0, & |u| \leq 1, \\ p_0 + p'_0 H_{mn}(u + 1), & u < -1, \end{cases} \quad (30)$$

where $p_0 = p^0(V_{mn})$ and $p'_0 = (dp^0/dV)$ just outside the shoulder of the island. Then from Eq. (28),

$$p(\psi) \simeq \begin{cases} p_0 + p'_0 H_{mn} \{ [(\psi_{mn}^0 + \psi_{mn}^1 - \psi)/2\psi_{mn}^1]^{1/2} - 1 \}, & \text{outer edge,} \\ p_0, & \text{inside island,} \\ p_0 + p'_0 H_{mn} \{ 1 + [(\psi_{mn}^0 + \psi_{mn}^1 - \psi)/2\psi_{mn}^1]^{1/2} \}, & \text{inner edge.} \end{cases} \quad (31)$$

This profile, which is illustrated in Fig. 1, is a reasonable approximation if there is negligible heating within the island so that the pressure profile there is flat.

Now average $p(\psi)$ over the poloidal (or toroidal) angle at fixed V to determine the background axisymmetric pressure profile to be used to calculate the coefficients in Eqs. (18) and (20):

$$p^0(V) = \int_0^{2\pi} \frac{d\theta}{2\pi} p(\psi). \quad (32)$$

After some algebra, it can be shown that^{23,28}

$$\begin{aligned} \frac{dp^0(V)}{dV} &\approx p'_0 |u| \frac{2}{\pi} \int_0^{\phi_m} \frac{d\phi}{(u^2 + \cos^2 \phi)^{1/2}} \\ &= p'_0 \frac{|u|}{(1+u^2)^{1/2}} \frac{2}{\pi} F[\phi_m, (1+u^2)^{-1/2}], \end{aligned} \quad (33)$$

where

$$\phi_m = \sin^{-1} [\min(1, |u|)], \quad (34)$$

and F stands for the elliptic integral of the first kind.²⁹ From numerical quadrature of Eq. (33) it can be shown that a reasonably good approximation is

$$\frac{dp^0(V)}{dV} \approx p'_0 \begin{cases} 0.63u^2, & |u| < 1, \\ 1 - 0.17/|u|, & |u| \geq 1. \end{cases} \quad (35)$$

(Note the discontinuity at $|u| = 1$.) It can be seen that the presence of a magnetic island makes dp^0/dV and d^2p^0/dV^2 both zero at the mode-rational surface. We refer to this region as a flat spot in the pressure profile. Because of this effect, the last term in Eq. (20) [using Eqs. (18) and (24)] goes like

$$\begin{aligned} \frac{p_{mn}^1}{nB^{0\zeta} - mB^{0\theta}} &= \frac{-iB_{mn}^{1V} dp^0/dV}{(nB^{0\zeta} - mB^{0\theta})^2} \rightarrow \frac{-iB_{mn}^{1V} p'_0 0.63}{[nB^{0\theta}(dq/dV)H_{mn}]^2}, \end{aligned} \quad (36)$$

at the mode-rational surface.

Now consider the current profile. At each mode-rational surface where there is a magnetic island with nonzero width, the presence of that island locally flattens the pressure profile so that the plasma is locally force-free ($\mathbf{J} \times \mathbf{B} = 0$ or $\mu_0 \mathbf{J} = K \mathbf{B}$). From $\nabla \cdot \mathbf{J} = 0$ and $\nabla \cdot \mathbf{B} = 0$, it follows that $\mathbf{B} \cdot \nabla K = 0$ and

$$\mu_0 J^\zeta / B^\zeta = \mu_0 J^\theta / B^\theta = K(\psi) \quad (37)$$

within this force-free region. It is clear that the first apparently singular term on the right-hand side of Eq. (20),

$$(nJ^{0\zeta} - mJ^{0\theta}) / (nB^{0\zeta} - mB^{0\theta}) = J^{0\zeta} / B^{0\zeta}, \quad (38)$$

remains finite at the mode-rational surface.

In order to determine the effect of the magnetic island on $d(\mu_0 J^{0\zeta} / B^{0\zeta}) / dV$, which appears in the second term on the right-hand side of Eq. (20), suppose the force-free current may be mildly peaked or suppressed within the magnetic island, so that $K(\psi)$ locally has the form

$$K \approx \begin{cases} K_0 + K_1(-1-u), & u \leq -1, \\ K_0 - \gamma K_1(1-u^2), & -1 \leq u \leq 1, \\ K_0 + K_1(1-u), & 1 \leq u, \end{cases} \quad (39)$$

through the widest part of the island ($m\theta - n\zeta = 0$). Here K_0 , K_1 , and γ are constants that are determined by the local current profile. These constants could be determined from the three-dimensionally flux-surface-averaged Ohm's law if the local resistivity and induced electric field were known from transport considerations. If the local Ohm's law were used, we would need to allow for the fact that the electric

field consists of an electrostatic part because of local charge separation in the neighborhood of the island as well as an inductively driven part. In order to avoid computing the electrostatic contribution to the electric field or computing the flux surface average within each island structure, we have avoided explicitly using Ohm's law in this model.

Repeating the kind of analysis carried out between Eqs. (30) and (34), we find

$$\begin{aligned} \frac{d}{dV} \left(\frac{\mu_0 J^{0\zeta}}{B^{0\zeta}} \right) &\approx \frac{K_1}{H_{mn}} \frac{|u|}{(1+u^2)^{1/2}} \frac{2}{\pi} F[\phi_m, (1+u^2)^{-1/2}] \\ &\quad + \frac{\gamma K_1 u \cos^{-1}(2u^2 - 1)}{H_{mn} \pi}, \end{aligned} \quad (40)$$

where $u_m = \min(1, |u|)$. Then for $|u| \ll 1$,

$$\frac{d(\mu_0 J^{0\zeta} / B^{0\zeta}) / dV}{nB^{0\zeta} - mB^{0\theta}} = \frac{2K_1(\gamma - u + \dots)}{H_{mn}^2 nq'(V)B^{0\theta}}. \quad (41)$$

This part of the contribution to Eq. (20), resulting from current peaking ($\gamma > 0$, assuming $K_1 < 0$) or current suppression ($\gamma < 0$) within the magnetic island, remains non-zero at the mode-rational surface, while the contribution resulting from the slope of the current profile off the shoulders of the island goes to zero at the mode-rational surface. In any event, the presence of a magnetic island removes the apparent singularity from Eq. (20) so that the ordinary differential equations (11) and (20) can be integrated right through each mode-rational surface.

It is now possible to describe an iterative algorithm for the determination of saturated tearing mode island widths in toroidal geometry. Start with an initial set of magnetic island widths for the resonant helical harmonics being considered. Determine the effect of these magnetic islands on the axisymmetric profiles, using Eqs. (33)–(41) in the neighborhood of mode-rational surfaces matched to the profiles determined by transport between magnetic islands. Solve for the new axisymmetric equilibrium to determine the Hamada coordinate metric elements for use in Eqs. (21) to (23) as well as the surface quantities $B^{0\theta}$, $B^{0\zeta}$, $J^{0\theta}$, $J^{0\zeta}$, and J . Then solve the ordinary differential equations (11) and (20) for the helical harmonics ($-iJB_{mn}^{1V}$, $B_{\theta mn}^1$) being considered, using Eqs. (18) and (19) and Fourier harmonics of Eqs. (21) to (23) to eliminate p_{mn}^1 , $B_{\zeta mn}^1$, $B_{V mn}^1$, $B_{mn}^{1\theta}$, and $B_{mn}^{1\zeta}$.

In general, no solution to Eqs. (11) and (20) with continuous first derivative satisfies the boundary condition $B_{mn}^{1V} = 0$ at both the magnetic axis (for $m \geq 2$) and at a perfectly conducting wall or infinity. If a saturated steady-state set of tearing modes exists, however, solutions can be found by suitably adjusting the magnetic island widths, determining their effect on the axisymmetric equilibrium and, consequently, their effect on the coefficients of Eqs. (11) and (20). Through this nonlinear process, the island widths act like eigenvalues for the differential boundary-value equations. Experience with the circular cylinder limit of the same equations²³ indicates that solutions can be obtained even when many helical harmonics are considered simultaneously. Interaction between magnetic islands can be highly non-

linear, since each island alters the axisymmetric background equilibrium and, therefore, the coefficients for all the other helical harmonics. Examples have been found where the solution is not unique.

IV. RESULTS

Equations (11) and (20) along with the island modification algorithm have been incorporated into a computer program called GTOR²⁸ to determine saturated magnetic island widths. The results presented in this section are obtained by starting with a consistent background axisymmetric equilibrium, modifying a parameter such as island current profile, and letting the computer algorithm find a neighboring three-dimensional equilibrium from this two-dimensional starting equilibrium. The background axisymmetric equilibrium is obtained by taking variational moments of the inverse Grad-Shafranov equation³⁰ and then converting this representation of the magnetic and current density fields to a Hamada representation. The $d(J^{0\zeta}/B^{0\zeta})/dV$ term is explicitly modified in the equilibrium algorithm in accordance with Sec. III of this paper. In the actual equilibrium computation, $d[J^{0\zeta}/B^{0\zeta}]/dV \equiv K'(q)$ is represented as a function of q (where $q = B^{0\zeta}/B^{0\theta}$ is the inverse rotational transform) so the flat spots on the current profile induced by magnetic islands are self-centered on each mode-rational surface (where $q = m/n$).

In this section we will determine the influence of various parameters on the width of saturated tearing mode magnetic islands in force-free equilibria ($\nabla p = 0$ throughout the plasma). In particular we will study the effect of (1) the breadth of the global current profile, (2) local peaking or suppression of current within the magnetic island being considered, (3) toroidal aspect ratio, (4) elongation of the plasma cross section, (5) harmonic coupling caused by toroidicity and elongation, and (6) the influence of multiple magnetic islands on each other through the background current profile.

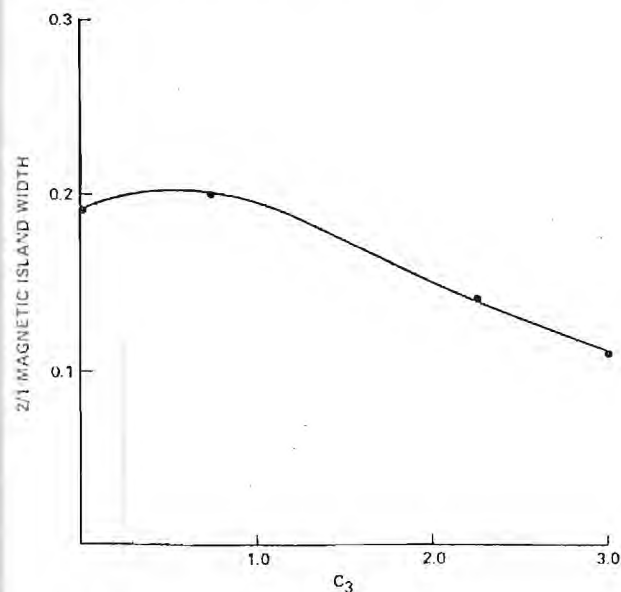


FIG. 2. Width of an $m/n = 2/1$ magnetic island relative to the plasma minor radius as a function of the current-peaking parameter C_3 .

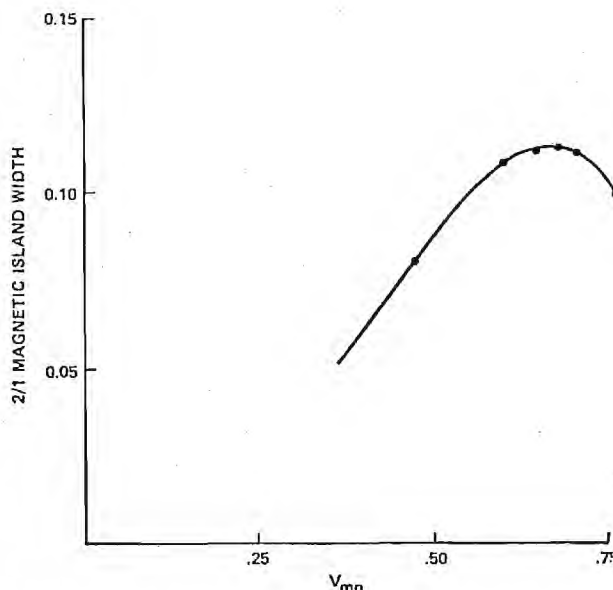


FIG. 3. Width of an $m/n = 2/1$ magnetic island relative to the plasma minor radius as a function of the minor radius position of the mode-rational surface.

The first parameter to be examined in the context of magnetic island widths is the effect of the shape of the background current density profile; in particular we are interested in the influence of "rounded" versus "peaked" current density profiles. This study was accomplished by varying the form of $K'(q)$ to produce a set of profiles that had the current increasingly "peaked" or concentrated near the magnetic axis. The trend produced was a reduction in the width of the magnetic island as the profile became more highly peaked in a way qualitatively similar to Ref. 25. This reduction in magnetic island width is not, in general, monotonic, and should be viewed in the light of the discussion of magnetic island current profiles.

In the cases presented the plasma parameters are aspect ratio = 4.0, elongation = 1.0, and a flat current profile within the island. In all cases the q on the magnetic axis was set equal to 1.0 because much lower values are not representative of most tokamak discharges. Figure 2 details the $2/1$ magnetic island width versus C_3 , where $K'(q) \equiv d(J^{0\zeta}/B^{0\zeta})/dV$ has the form $K'(q) = C(C_0 + C_1x + C_2x^2 + C_3x^3)^{1/2}$; where C_0, C_1, C_2 , and C_3 are parameters that are used to characterize an equilibrium, C is selected by the equilibrium subroutine to satisfy the condition of zero current at the plasma edge, and $x \equiv (q - q_{\text{axis}})/(q_{\text{edge}} - q_{\text{axis}})$. In this case $C_0 = 1.0$, $C_1 = 0.3$, $C_2 = 0.0$, and C_3 was varied to produce various equilibria. As C_3 is increased, the q at the plasma edge increases and the current density profile becomes more highly concentrated near the magnetic axis. As the current density becomes more highly peaked at the center of the plasma, the mode-rational surface shifts inward. Figure 3 shows the magnetic island width versus the position of the mode-rational surface. In general, it appears that the more "rounded" current density profiles with the low q values at the plasma edge are the profiles that are the most unstable to tearing modes.

The effect of local current peaking or suppression within

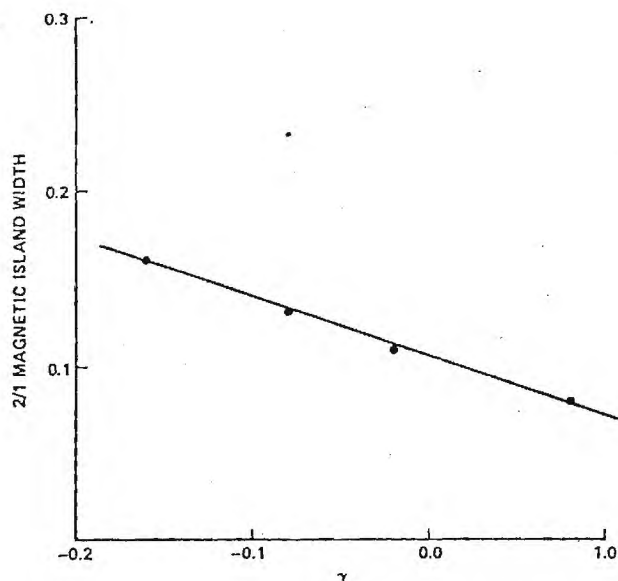


FIG. 4. Relative width of an $m/n = 2/1$ magnetic island as a function of the current peaking parameter γ defined in Eq. (39).

magnetic islands can be studied in a parametric manner by varying gamma in Eqs. (39) and (40). Figure 4 is a plot of the 2/1 magnetic island width versus γ ; note that as gamma increases, the magnetic island width decreases over a range of about 60%. The plasma parameters for this study were aspect ratio = 4.0, elongation = 1.0, $C_0 = 1.0$, $C_1 = 0.5$, $C_2 = 0.0$, and $C_3 = 1.25$. Since K_1 is negative, a positive gamma corresponds to a current density profile peaking within the magnetic island, while a negative gamma corresponds to a current density profile dip within the island. Of special interest is the observation that a negative γ can destabilize an otherwise stable island. Figure 5 illustrates this behavior with a 3/2 island. The plasma parameters in this case were aspect ratio = 4.0, elongation = 1.0, $C_0 = 1.0$, $C_1 = 0.0$, $C_2 = 0.0$, and $C_3 = 0.5$.

It is useful to estimate the magnitude of the possible

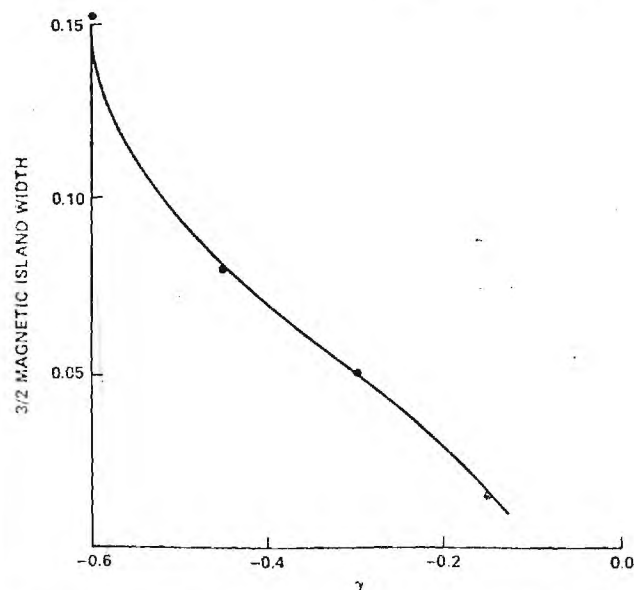


FIG. 5. Relative width of an $m/n = 3/2$ magnetic island as a function of the current peaking parameter γ defined in Eq. (39).

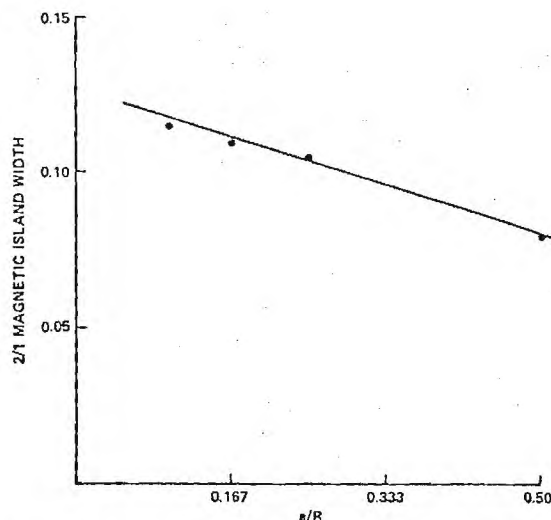


FIG. 6. Relative width of an $m/n = 2/1$ magnetic island as a function of the inverse aspect ratio.

current peaking within an island; if the current density gradient within a magnetic island is the same order of magnitude as that in the plasma proper, γ could have values between -1.0 and 1.0 . Thus while the current peaking is moderate, the fact that $K'(q)/(nq - m)$ is no longer zero at the mode-rational surface is of great consequence. This implies that the second derivative of the current density profile is important near the mode-rational surface.

Equation (20) is a relationship involving both the contravariant and covariant vector components, and one would expect harmonic mixing when converting from one form to another; Eqs. (21)–(23) detail this conversion. The metric elements provide cross-harmonic driving terms and modes with the same n number may influence each other through this coupling. The principal coupling elements are toroidicity and plasma elongation, both of which are expected to be present in future tokamaks. Figure 6 shows the 2/1 magnetic island width versus inverse aspect ratio, and Fig. 7 shows the

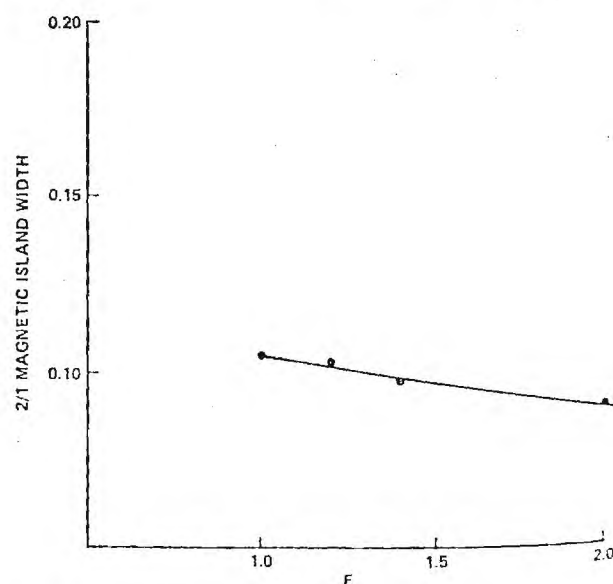


FIG. 7. Relative width of an $m/n = 2/1$ magnetic island as a function of the elongation of the plasma cross section.

1 magnetic island width versus elongation. In both of these graphs, the q on axis remained fixed at 1.0, $C_0 = 1.0$, $C_1 = 0.5$, $C_2 = 0.0$, $C_3 = 1.25$, and the current profile within the magnetic island was flat. With the method of equilibrium computation used it was not possible to keep the q at the edge of the plasma constant. It increased both with a decrease in aspect ratio and an increase in elongation, and thus the family of equilibria generated differs somewhat in the magnetic island configuration as well as the aspect ratio. The effects of toroidicity and elongation on the magnetic island width depend on the position of the magnetic island to some degree, being somewhat greater for islands nearer the edge of the plasma where the metric elements have the strongest dependence on θ ; however, again this is profile dependent. The effect of toroidicity is to reduce the saturated magnetic island width as the aspect ratio decreases; this is qualitatively consistent with Ref. 19. As the aspect ratio was decreased, the mode-rational surface receded into the plasma. Since the form of the current density profile changed as the aspect ratio changed, it being dependent upon the specific equilibrium solution, there may be some question as to whether the toroidicity causes the current density profile to change. This might cause the reduction in magnetic island width, rather than a direct connection between the island width and toroidicity. Plasma elongation also appears to reduce the saturated magnetic island width, but care should be taken when interpreting these results since the equilibrium current density profile changes radically with large changes in plasma elongation. As the elongation increases the mode-rational surface also shifts inward as in the toroidal case, but to a lesser extent. With either current peaking, toroidicity, or elongation, a reduction in the magnetic island width has generally been associated with the inward shift of the mode-rational surface. Since this inward shift of the mode-rational surface cannot be separated from the equilibrium computations used in this model, a further examination of elongation and toroidicity with a global plasma transport model would be a useful extension of this work.

Mode mixing occurs when perturbations of the same n number interact through metric element coupling to enhance or suppress each other and thus modify the magnetic island widths. In the cases studied, the effect of the 2/1 island on the 3/1 island was examined, and it was found that the 2/1 island could drive a 3/1 island in equilibria that would not otherwise support a 3/1 island, provided that there was a large amount of plasma elongation present. With only small amounts of elongation no effects could be detected. Even with large amounts of elongation the 3/1 island width was only about 1% of the minor radius and the 2/1 magnetic island remained essentially the same. In this case the plasma parameters were aspect ratio = 4.0, elongation = 2.0, and $(q) = \text{const}$. The aspect ratio had only a minor effect on mode mixing in the cases studied.

Unlike some work done using the time-dependent MHD equations,¹⁸ the 1/1 mode could not be generated (because in general it oscillates in time and does not saturate) and thus what may be the major harmonic driving term could not be modeled in the present study. Another difference is that the magnetic island is allowed to modify the

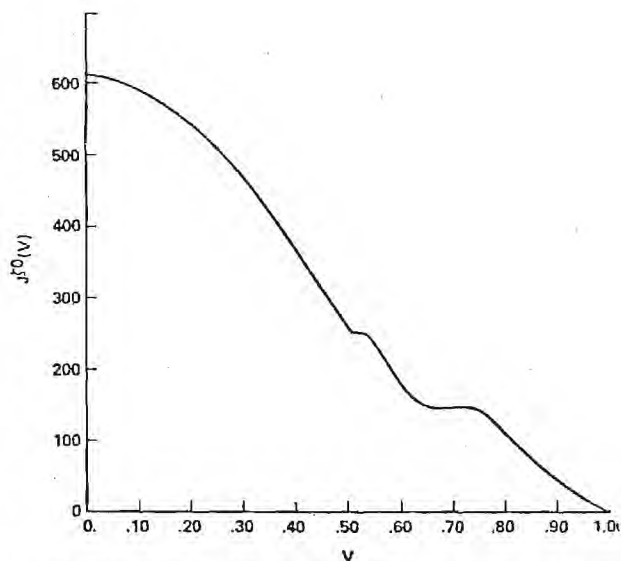


FIG. 8. Current density profile as a function of relative minor radius showing the combined effects of $m/n = 3/2$ and $2/1$ magnetic islands.

background current density profile in the model of this paper, while the background resistivity remained only a function of the radial coordinate rather than a function of the magnetic surfaces in the work of Refs. 16 and 17. This may result in differences in the functional form of the perturbed radial magnetic field components.

The effect of two magnetic islands of different helicity n numbers coupling through the background current density profile can be of great importance. When a magnetic island exists, it modifies the background current profile and in some cases may radically steepen the current gradients on either side of it, thereby nonlinearly coupling to and destabilizing nearby islands. This type of behavior can be illustrated by examining the interaction of the 3/2 and 2/1 magnetic islands. When the 3/2 island is present, the 2/1 magnetic island is found to be larger than it was without the 3/2 island. The width of the 3/2 island is approximately the same as before the inclusion of the 2/1 island, but its presence modifies the current density gradient between the two islands. Figure 8 shows the current density profile for a case of this type. As the current density suppression in the 2/1 island is increased, the combination of current density gradient destabilization and current density suppression causes a large increase in the width of the 2/1 island and a small reduction in the width of the 3/2 island. The total region occupied by magnetic island increases, however. The net result is that the two islands begin to coalesce as the coupling increases and the background equilibrium current density profile suffers a high degree of modification by the islands—a ledge begins to appear in the plasma middle region. The locations of the mode rational surfaces seem to be important—the closer they are the greater the coupling. The plasma parameters were aspect ratio = 4.0, elongation = 1.0, $C_0 = 1.0$, $C_1 = 0.0$, $C_2 = 0.0$, and $C_3 = 0.50$. The nonlinear coupling demonstrated by this model shows the importance of the phenomenon; it is interesting to note that one scenario for the major disruption is the interaction of the 3/2 and 2/1 islands, which may overlap and destroy a major portion of the plasma confinement volume.¹³

V. CONCLUSIONS

The quasilinear model has proven to be useful in the computation of saturated magnetic island widths. Unlike the reduced MHD equations, the quasilinear equations consider only the asymptotic time limit and thus do not follow the evolution of the equilibrium as a function of time. They can, however, handle cases of greater geometric complexity within a reasonable computing time limit, and this feature, along with a somewhat simpler equation set, is their source of attraction. One major limitation is the inability of the equations to model tearing modes that undergo relaxation oscillations in time, such as the $m = 1/n = 1$ mode.

In the course of the derivation of the quasilinear equations, it has been shown that the magnetic island influences the background current density profile. Using a simple approximation for the pressure and current density within a magnetic island, the effect of the magnetic island on the background equilibrium has been quantified and a self-consistent set of equations formed. This set of equations has been solved for a variety of parameters, including toroidicity, plasma elongation, equilibrium current density profile, and current density profile within a magnetic island. The results of greatest interest are the effects of the current density profile within a magnetic island.

The most unexpected effect is the fact that suppression of the current density profile within a magnetic island can cause a large increase in the width of a magnetic island and can also destabilize otherwise stable magnetic islands. This result suggests a possible means of magnetic control: to locally heat the plasma or drive current within each magnetic island in order to increase the current density there and reduce the island width.

The nonlinear coupling of magnetic islands through the background current density profile has been found to increase the saturated width of magnetic islands when the current density gradient at the inner edge of the island is increased by the presence of another magnetic island. This effect is independent of the mode numbers of the islands involved and thus all the islands within a plasma will be coupled to a degree that depends on the relative spacing between the islands and the width of the islands themselves. Linear coupling of magnetic islands with the same n number occurs when toroidicity and/or elongation is present. This linear coupling can cause normally stable islands to be driven unstable by their unstable neighbors and thus increase the amount of the plasma that is occupied by magnetic islands. In the work done, however, this was found to be a minor effect, possibly because the $1/1$ magnetic island could not be included. When toroidicity and/or elongation is increased in a plasma with only a single mode present, the saturated magnetic island width showed a small decrease. In all the cases studied it was noted that, in general, the magnetic island width decreased as the mode rational surface shifted inward pointing to low q edge plasmas as being the most unstable to tearing modes.

Since the saturated magnetic island width and even its existence depends to a large extent on the local current density profile, knowledge of the global current density profile may not be sufficient to predict magnetic island behavior.

Unless the current density profile can be measured accurately or externally controlled, the prediction of the saturated magnetic island width may, by necessity, take on a probabilistic nature.

ACKNOWLEDGMENTS

It is a pleasure to acknowledge a number of stimulating discussions with Dr. B. A. Carreras.

This work was supported by the U. S. Department of Energy under contract No. DE-AS05-81ER53117 at the Georgia Institute of Technology.

- ¹M. N. Rosenbluth, D. A. Monticello, H. Strauss, and R. B. White, *Phys. Fluids* **19**, 1987 (1976).
- ²R. B. White, D. A. Monticello, and M. N. Rosenbluth, *Phys. Rev. Lett.* **39**, 1618 (1977).
- ³H. R. Strauss, *Phys. Fluids* **20**, 1354 (1977).
- ⁴B. V. Waddell, B. Carreras, H. R. Hicks, J. A. Holmes, and D. K. Lee, *Phys. Rev. Lett.* **41**, 1386 (1978).
- ⁵B. V. Waddell, B. Carreras, H. R. Hicks, and J. A. Holmes, *Phys. Fluids* **22**, 896 (1979).
- ⁶B. Carreras, B. V. Waddell, and H. R. Hicks, *Nucl. Fusion* **19**, 1423 (1979).
- ⁷H. R. Hicks, J. A. Holmes, B. A. Carreras, D. J. Tetreault, G. Berge, J. P. Freidberg, P. A. Politzer, and D. Sherwell, *Plasma Physics and Controlled Nuclear Fusion*, Eighth International Conference, Brussels (IAEA, Vienna, 1980), Vol. I, p. 259.
- ⁸A. Sykes and J. A. Wesson, *Phys. Rev. Lett.* **44**, 1215 (1980).
- ⁹B. Carreras, H. R. Hicks, J. A. Holmes, and B. V. Waddell, *Phys. Fluids* **23**, 1811 (1980).
- ¹⁰B. A. Carreras, J. A. Holmes, H. R. Hicks, and V. E. Lynch, *Nucl. Fusion* **21**, 511 (1981).
- ¹¹J. D. Callen, B. V. Waddell, B. Carreras, M. Azumi, P. J. Catto, H. R. Hicks, J. A. Holmes, D. K. Lee, S. J. Lynch, J. Smith, M. Soler, K. T. Tsang, and J. C. Whitson, in *Plasma Physics and Controlled Nuclear Fusion*, Seventh International Conference, Innsbruck (IAEA, Vienna, 1978), Vol. I, p. 415.
- ¹²K. Bol, V. Arunasalem, M. Bitter, D. Boyd, K. Brau, N. Bretz, J. Bussac, S. Cohen, P. Colestock, S. Davis, D. Dimock, F. Dylla, D. Earnes, P. Ethrington, H. Eubank, R. J. Goldston, R. J. Hawryluk, K. W. Hill, E. Hinnov, J. Hosea, H. Hsuan, F. Jobs, D. Johnson, E. Mazzucato, S. Medley, E. Mersurvey, N. Sauthoff, G. Schmidt, F. Stauffer, W. Stodiek, J. Strachan, S. Suckewer, G. Tait, M. Ulrickson, and S. Von Goeler, in Ref. 11, p. 11.
- ¹³K. Toi, K. Sakurai, S. Tanahashi, and S. Yasue, *Nucl. Fusion* **22**, 465 (1982).
- ¹⁴N. R. Sauthoff, S. Von Goeler, and W. Stodiek, *Nucl. Fusion* **18**, 1445 (1978).
- ¹⁵F. Karger, K. Lackner, G. Fussman, B. Cannici, W. Engelhardt, J. Gerhardt, E. Glock, D. E. Groening, O. Kluber, G. Lisitano, H. M. Mayer, D. Meisel, P. Morandi, S. Sessnic, F. Wagner, and H. P. Zehrfeld, in *Plasma Physics and Controlled Nuclear Fusion Research*, Sixth International Conference, Berchtesgaden (IAEA, Vienna, 1976), Vol. I, p. 267.
- ¹⁶H. R. Hicks, B. A. Carreras, J. A. Holmes, D. K. Lee, and B. V. Waddell, *J. Comput. Phys.* **44**, 46 (1981).
- ¹⁷J. A. Holmes, B. A. Carreras, T. C. Hender, H. R. Hicks, V. E. Lynch, and E. F. Masden, *Phys. Fluids* **26**, 2569 (1983).
- ¹⁸J. L. Dunlap, B. A. Carreras, V. K. Pare, J. A. Holmes, S. C. Bates, J. D. Bell, H. R. Hicks, V. E. Lynch, and A. P. Navarro, *Phys. Rev. Lett.* **48**, 538 (1982).
- ¹⁹R. Izzo, D. Monticello, W. Park, J. Manickam, H. R. Strauss, R. Grimm, and K. McGuire, *Phys. Fluids* **26**, 2240 (1983).
- ²⁰S. Hamada, *Nucl. Fusion* **2**, 23 (1962).
- ²¹J. M. Greene and J. L. Johnson, *Phys. Fluids* **5**, 510 (1962).
- ²²G. Bateman, *MHD Instabilities* (MIT, Cambridge, MA 1978).
- ²³See AIP document no. PAPS PFLDA-29-0753-37 for 37 pages of Georgia Tech. Fusion Report GTFR-15. Order by PAPS number and journal reference from American Institute of Physics, Physics Auxiliary Publication Service, 335 East 45 Street, New York, NY 10017. The price is \$1.50 for each microfiche (98 pages) or \$5.00 for photocopies of up to 30 pages, and \$50.15 for each additional page over 30 pages. Airmail additional. Make

checks payable to the American Institute of Physics.

²⁴W. Kerner and H. Tasso, *Plasma Phys.* **24**, 97 (1982).

²⁵R. B. White, D. A. Monticello, M. N. Rosenbluth, and B. V. Waddell, *Phys. Fluids* **20**, 800 (1977).

²⁶A. Sykes and J. A. Wesson, in Ref. 7, p. 237.

²⁷L. S. Solov'ev and V. D. Shafranov, *Reviews of Plasma Physics* (Consul-

tants Bureau, New York, 1970), Vol. 5, p. 1.

²⁸R. N. Morris, Ph.D. thesis, Georgia Institute of Technology, 1984.

²⁹I. S. Gradshteyn and I. M. Ryzhik, *Table of Integrals, Series, and Products* (Academic, New York, 1965), Secs. 8.11 and 8.12.

³⁰L. L. Lao, S. P. Hirshman, and R. M. Weiland, *Phys. Fluids* **24**, 1431 (1981).